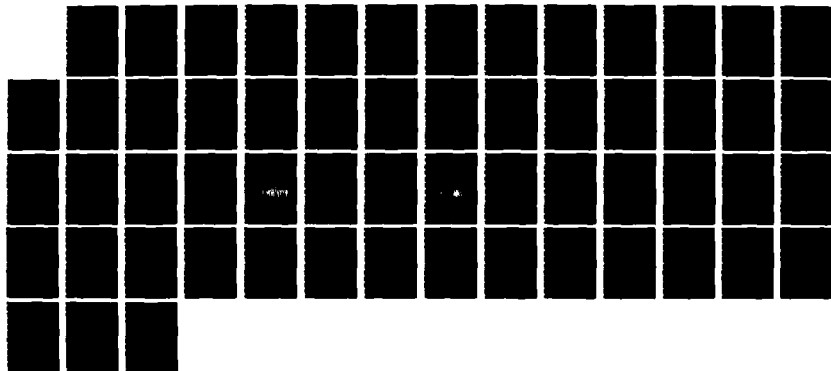


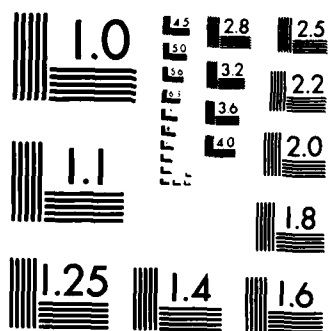
AD-A172 553 ADVANCED COMPUTATIONAL TECHNIQUES FOR POWER TUBE DESIGN 1/1
(U) VARIAN ASSOCIATES INC PALO ALTO CA PALO ALTO
MICROWAVE TUBE DIV JUL 86 N00014-86-C-2074

UNCLASSIFIED

F/G 9/1

NL





MICROCOPY RESOLUTION TEST CHART
NATIONAL BUREAU OF STANDARDS-1963-A

AD-A172 553

2



ADVANCED COMPUTATIONAL TECHNIQUES FOR POWER TUBE DESIGN

PHASE I FINAL REPORT

PREPARED FOR:
NAVAL RESEARCH LABORATORY
WASHINGTON, D.C. 20375

CONTRACT N00014-86-C-2074

JANUARY 1986 - JULY 1986

REPORT DATE
JULY 1986

This report is the property of the
Naval Research Laboratory and its
distribution is unlimited.

DTIC
OCT 3 1986

Varian Associates, Inc.
Palo Alto Microwave Tube Division
611 Hansen Way
Palo Alto, California 94303

DTIC FILE COPY

86 8 11 031
031

PHASE I - FINAL REPORT

PART I

VARIAN ASSOCIATES, INC.

PHASE I FINAL REPORT:

ADVANCED COMPUTATIONAL TECHNIQUES FOR POWER-TUBE DESIGN

Update of Program Plan Outline

PHASE 2:

Varian will perform or make significant contributions to the following task:

- A. Provide guidance as necessary to MRC in the areas of
 - o User-friendliness of code
 - o Data input to/output from code
 - o RF cold-test methods

PHASE 3:

Varian will perform or make significant contributions to the following tasks:

- A. Implement code at Varian. Check program using case run by MRC in Phase 2. Apply code to actual tube problems to exercise as many code features as possible.
- B. Provide feedback to MRC, based on user experience, for update of code. Participate in some of the updating effort in areas of special expertise.
- C. Perform final validation of code (and verification of user-friendliness). Initiate reiteration of upgrade/verification cycle if necessary.
- D. Assist in preparation of final report and users' manual, particularly where dealing with application of code to tube problems and its validation using actual cold-test data. Assemble final version of final report. (MRC will provide final version of users' manual and program documentation plus a list of the input required to repeat the SPS calculations, along with their results, and a sequence of sample problems for familiarizing users with code capabilities and failure modes. All code modifications will be documented.)



A-1

PHASE I FINAL REPORT:

ADVANCED COMPUTATIONAL TECHNIQUES FOR POWER-TUBE DESIGN

CAD, CAM and CAE at Varian

The Varian Microwave Tube Division (MTD), located in Palo Alto, CA, is the largest Division of the Electron Device Group (EDG). Through MTD and its other Divisions, EDG manufactures and markets microwave and radio-frequency electron tubes and solid-state devices.

MTD's CAD/CAM/CAE facilities are integrated with Management Information Systems (MIS), within the Division, and connected to mainframe computers at Corporate Headquarters in Palo Alto via a Local Area Network. Figure 1 schematically illustrates the major features of this computer network. The backbone of our system is a Sytek Broadband Network (LAN) which interconnects terminals and micro-, mini- and mainframe computers. Other terminals and PCs, used predominantly for Production Control, are connected directly to the mainframe IBM 3081.

The CAD system, illustrated in Figure 2, comprises two Computervision System D021 computers, with various peripherals, servicing a total of nine CAD stations -- one of which functions as the Numerical Machine Control Station. Drawings are reduced to programs on the Corporate Amdahl computer and downloaded to an IBM PC and controller (via the LAN) which drive the numerically controlled machines. The communication means for the CAD system includes a high-speed link (GNA) between the two Computervision systems, to expedite file transfer, and a LAN connection for accessing other Division and Corporate computer facilities.

Figure 3 illustrates the computer interconnections for the Division Automation Department which is responsible for integrating CAD/CAM/CAE/CIM activities within the Division. The Division's two VAX 750s and Corporate's IBM 3081 are indicated at upper left in the figure. These facilities support the needs of Management Information Systems and Production Control as well as fulfill the engineering uses to be described in more detail below.

At lower left in Figure 3 are indicated a terminal and Mass Comp and HP 1000 computers. The HP 1000 controls a microwave automatic network analyzer (FANA) which electrically characterizes the slow-wave helices of traveling-wave tubes (TWTs) -- both for engineering design purposes and as a means for controlling tube operating characteristics in Manufacturing. The Mass Comp computer provides high-speed A/D and D/A functions utilized in computer-controlled testing of TWT characteristics as required for engineering and design.

Figure 3 further includes, schematically at the right, four additional facilities:

- o The Research and Development Department employs microcomputers and terminals in conjunction with the VAX 750s and the IBM mainframe for a wide range of activities. These include device simulation for electrical, magnetic, thermal and mechanical design, and the generation of computer codes supporting these capabilities.
- o Klystron Manufacturing users employ the shared computer resources for failure and returned-product analyses and control in addition to computer-aided engineering. Installation of a tooling and fixturing data base is planned.
- o Communications Tube Manufacturing users are planning to implement programs for failure and returned-product analyses, and for tooling and fixturing applications, in addition to the existing computer-aided engineering capabilities.
- o Helix TWT Manufacturing has implemented a tooling and fixturing data base as well as computer-aided engineering facilities, and is planning to add means for failure and returned-product analyses. Integration of existing hot-test stations is also planned. Such a station is shown schematically in Figure 4. An existing automatic helix-winding facility will be integrated along with a magnet shop manufacturing rare-earth/cobalt magnets. Additional plans to create a comprehensive computer-integrated facility include incorporation of facilities for monitoring TWT exhaust and processing.

A proposed engineering/manufacturing data base (EMDB) is illustrated in Figure 5. In addition to the facilities already described it includes a Britton Lee hardware data-base machine to be used for maintaining interactive files covering all manufacturing, test and process data.

The EMDB will permit traceability in microwave tube manufacture. Its engineering portion will provide engineering records of design and performance for all tubes produced. Design parameters accumulated from past experience will be selectable via the relational data base. For example, an engineer required to design a tube with certain parameters can take advantage of past experience by retrieving a list of past designs matching the parameter list, selecting those closest to the current need and recalling engineering and production data. The Computervision files can then deliver the drawings which can be modified to provide the "new" design.

The manufacturing data base will use bar-code devices and interactive terminals to record data on material lots and fabrication processes as well as assembly instructions, test data and all activity relative to tubes in production. The files will be in a relational data base permitting management control of process, QA-analysis, yield and trend data. It will also allow analysis stations to develop statistical studies of production data. It is planned that data for all automated process and test systems be collected automatically.

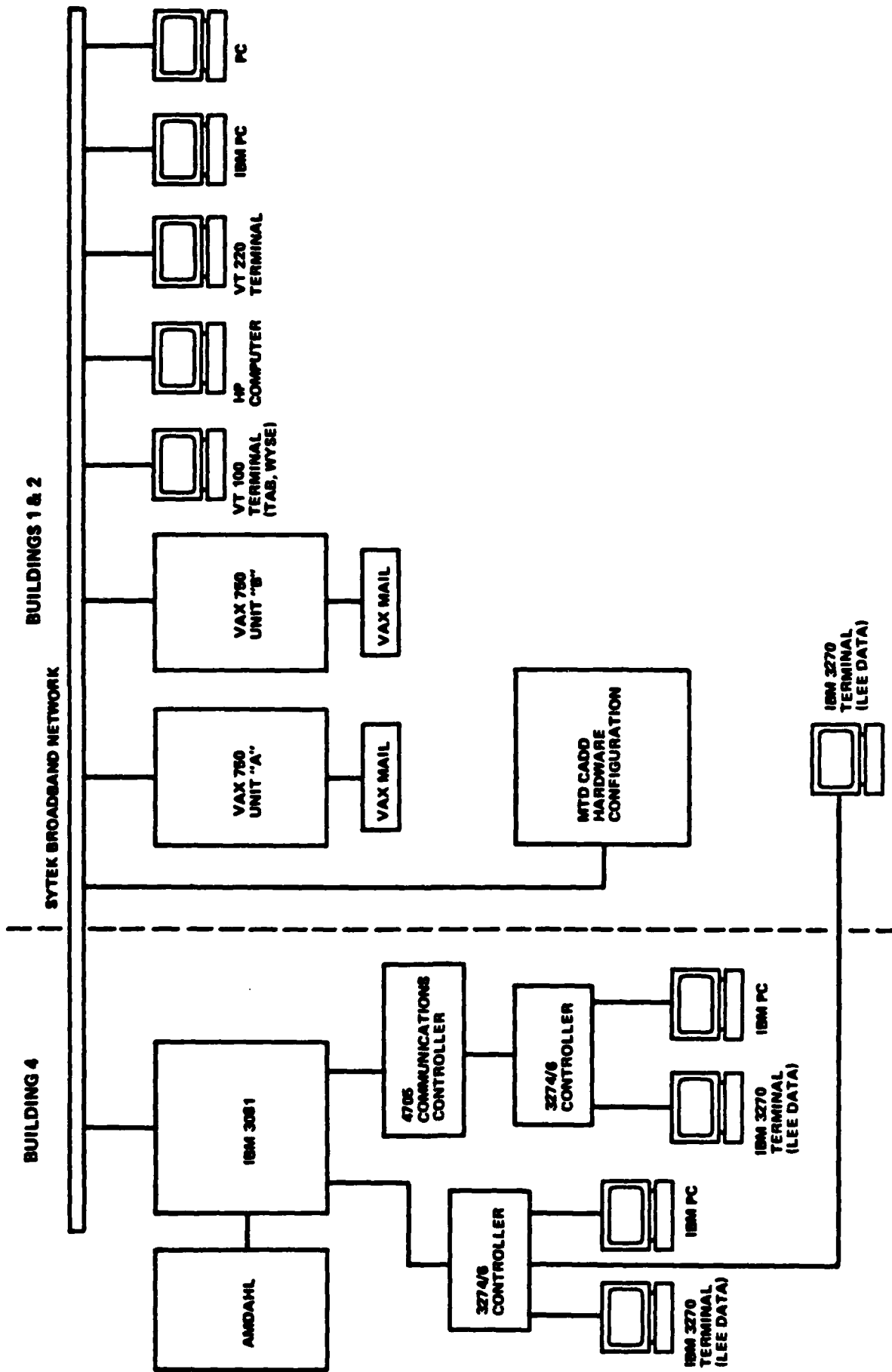


FIGURE 1. VARIAN DATA COMMUNICATION NETWORK

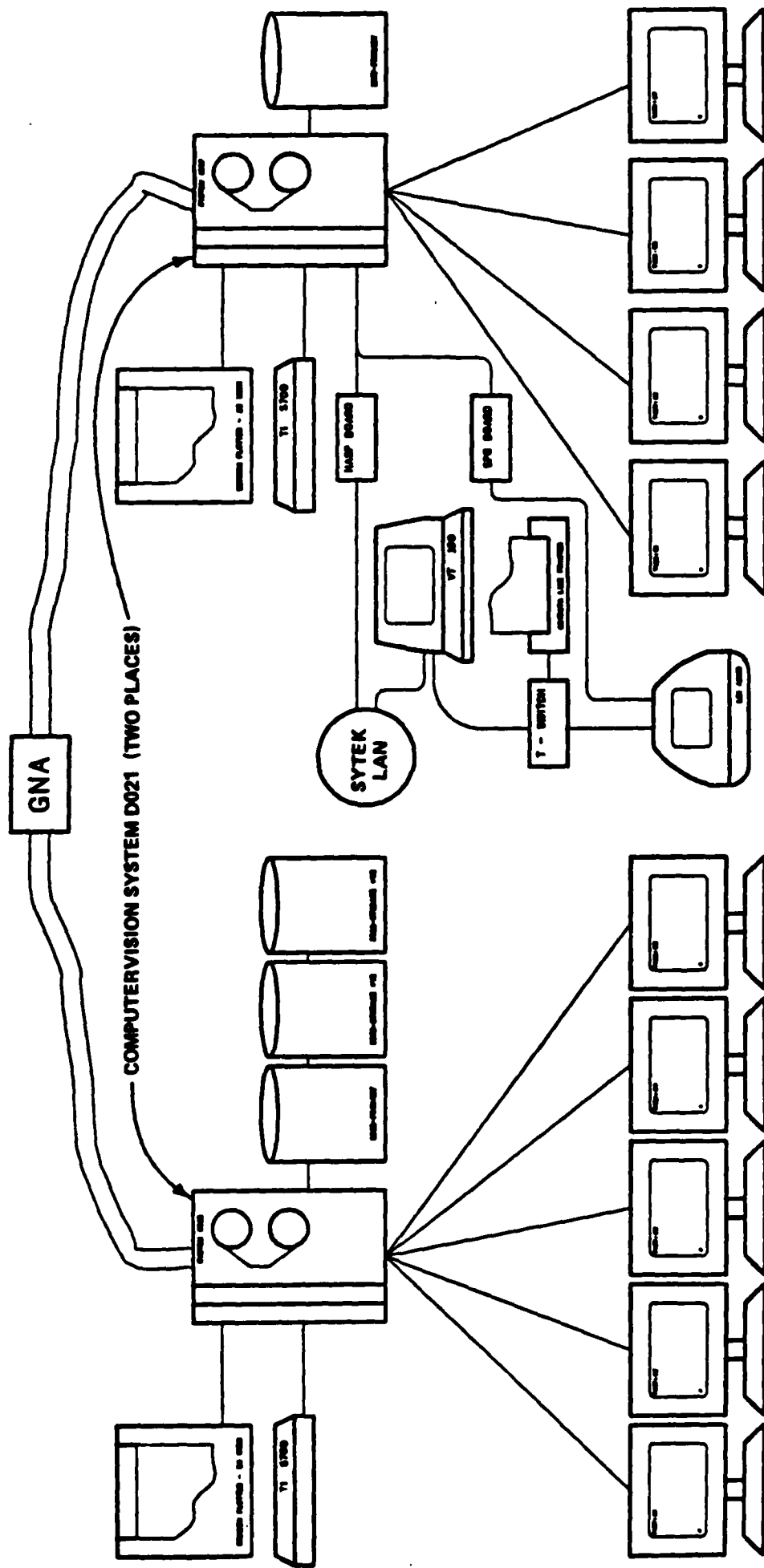
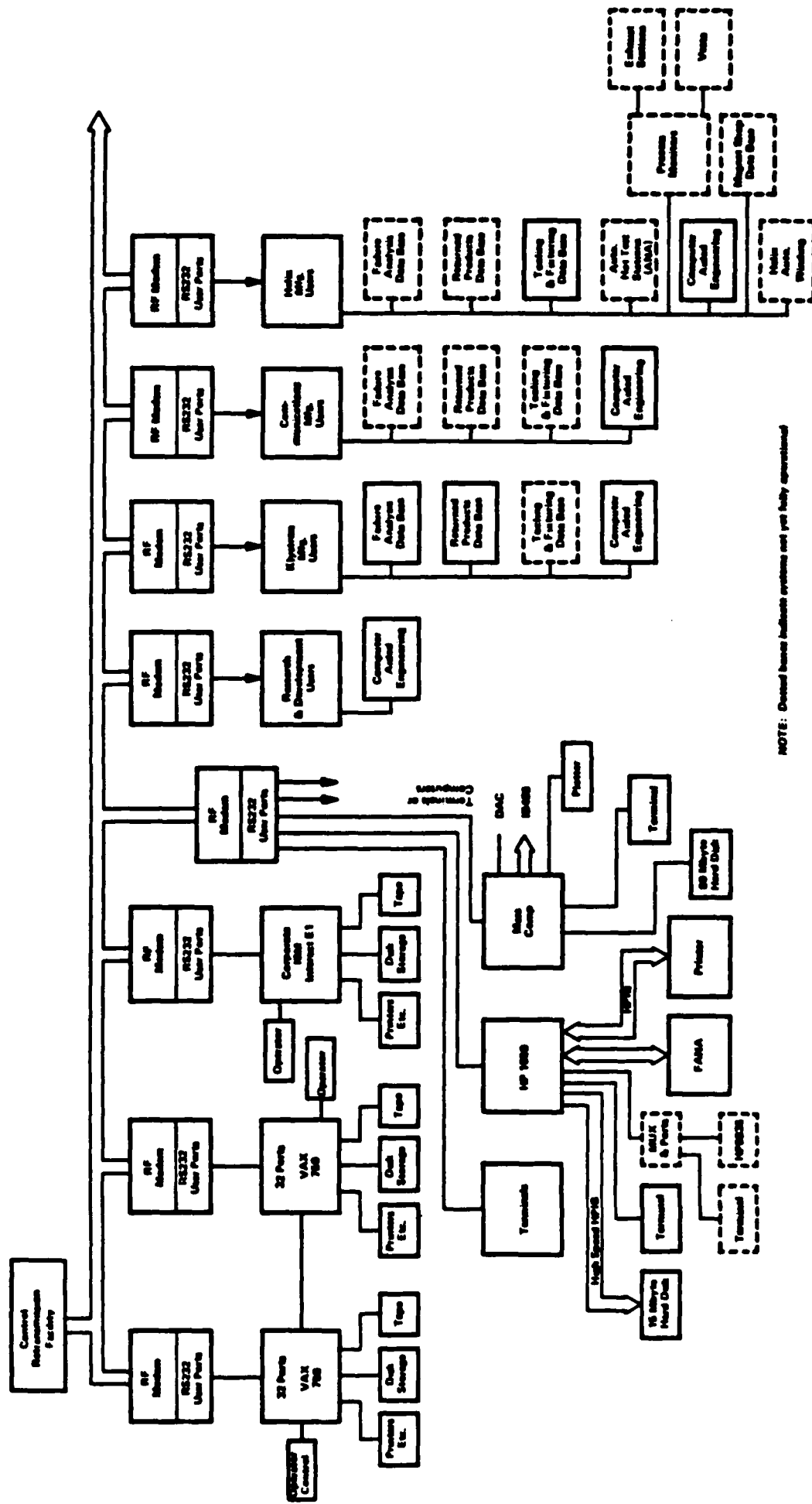


FIGURE 2. MTD - CADD HARDWARE CONFIGURATION



NOTE: Dashed boxes indicate systems not yet fully operational

FIGURE 3. AUTOMATION DEPARTMENT COMPUTER INTERCONNECTIONS

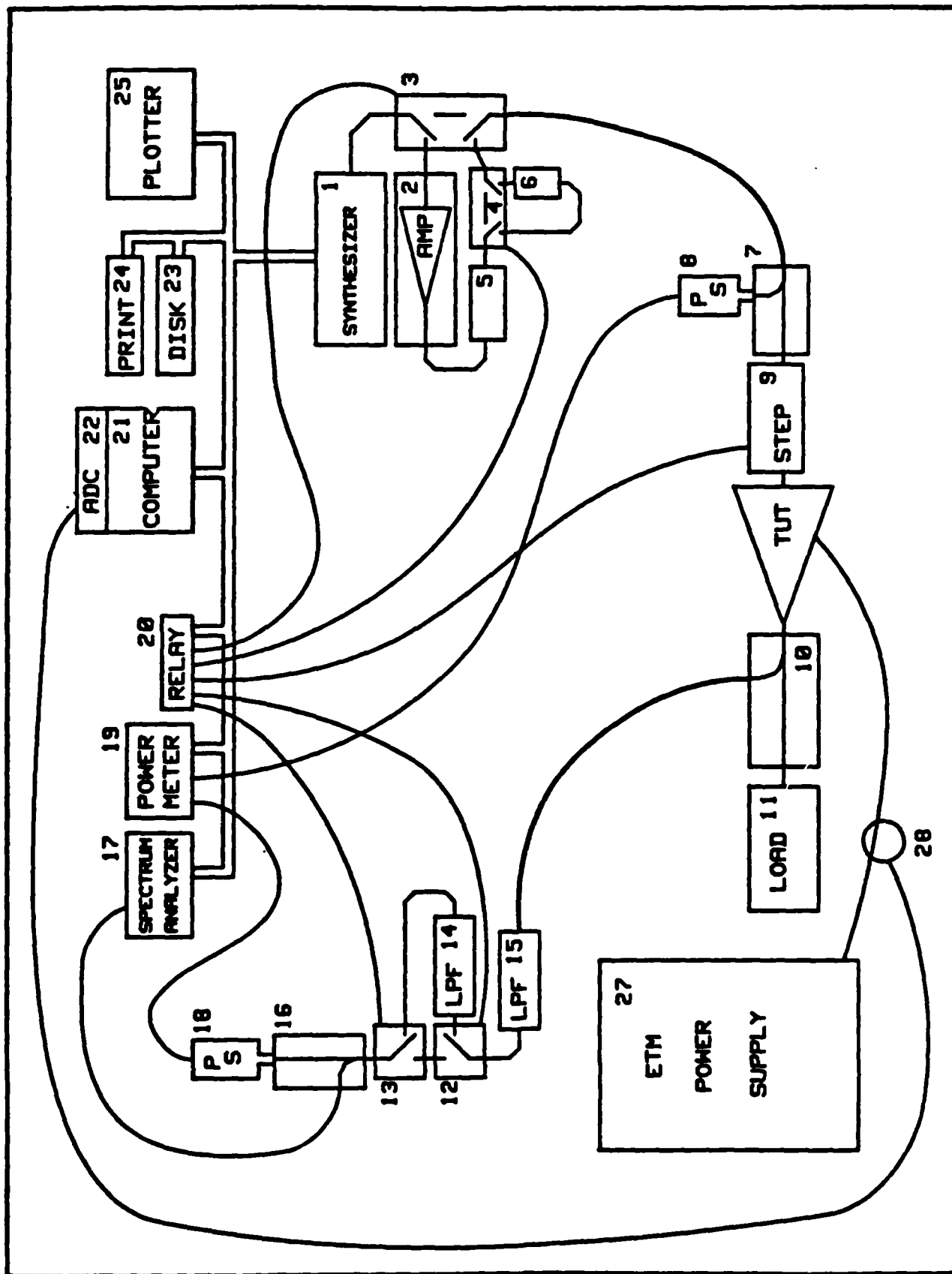


FIGURE 4. SCHEMATIC FOR TWT AUTOMATIC TEST SET

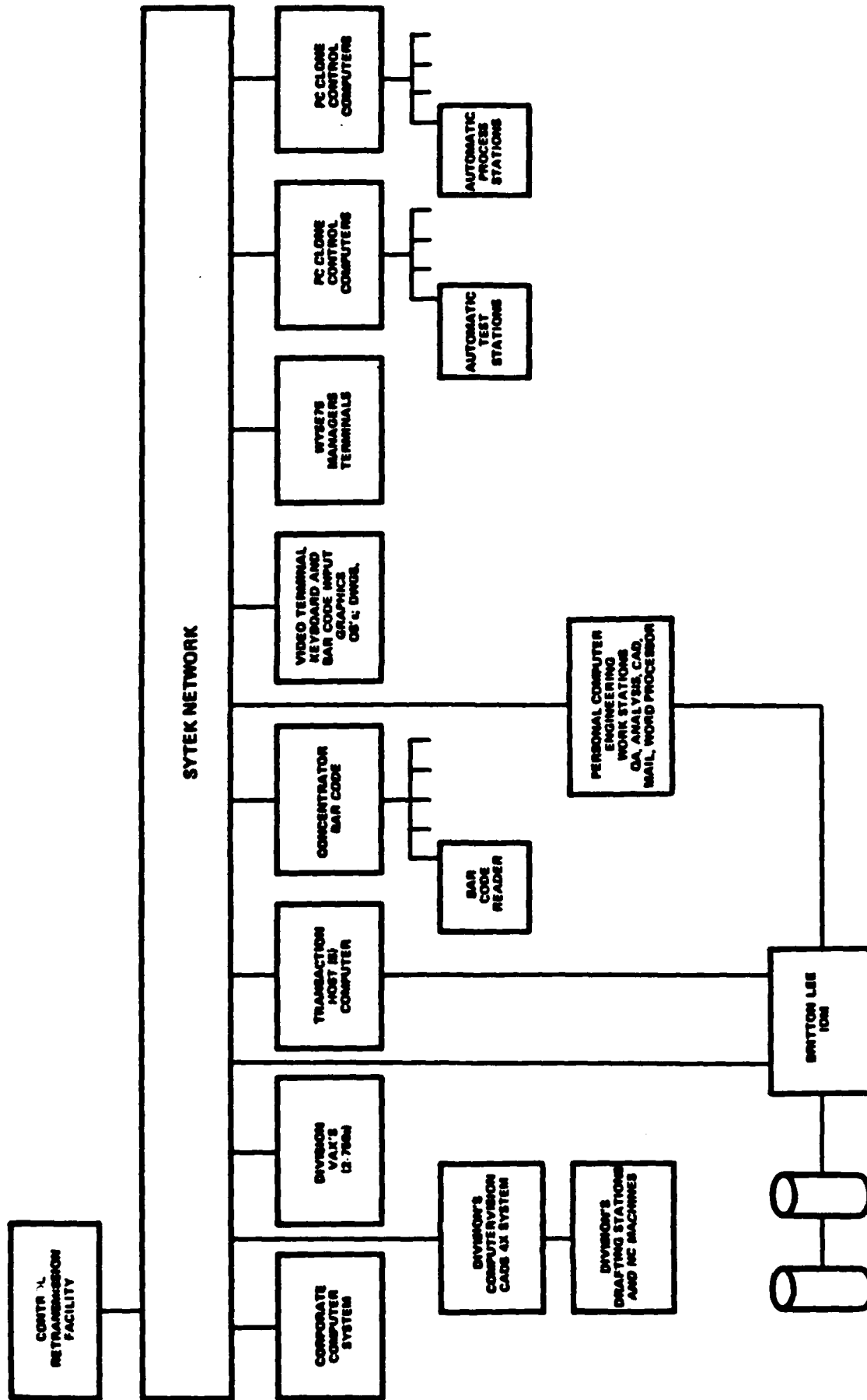


FIGURE 5. PROPOSED ENGINEERING/MANUFACTURING DATA BASE

PHASE I - FINAL REPORT

PART II

MISSION RESEARCH CORPORATION

COPY 1

MRC/WDC-R-113

COLD-TEST SIMULATION: PHASE I

Bruce Goplen
James McDonald

June 1986

Submitted to: Varian Associates, Inc.
611 Hansen Way
Bldg. 1, Mail Stop A-109
Palo Alto, CA 94303

Contract No: PO #10ABW161235

MISSION RESEARCH CORPORATION
5503 Cherokee Avenue, Suite 201
Alexandria, Virginia 22312
(703) 750-3556

CONTENTS

SECTION		PAGE
1	INTRODUCTION	1-1
	1.1 BACKGROUND	1-1
	1.2 DESCRIPTION OF THE PROGRAM	1-2
	1.3 PHASE 1 SUMMARY	1-2
2	COLD-TEST SIMULATION OF CCTWT	2-1
	2.1 DESCRIPTION OF THE SOS CODE	2-1
	2.2 SUB-GRID MODELS OF CABLE DRIVERS	2-2
	2.3 MODEL OF THE CCTWT	2-8
	2.4 CALCULATED RESULTS	2-11
3	PROGRAM PLAN	3-1
	3.1 KEY TECHNICAL ISSUES	3-1
	3.2 OVERVIEW OF PLANNED DESIGN SYSTEM	3-2
4	REFERENCES	4-1

LIST OF FIGURES

FIGURE		PAGE
1	Geometry for Cable Models	2-4
2	CCTWT Model Geometry and Dimensions	2-9
3	Axial Electric Field Near Beam in Symmetric, Unmodified CCTWT	2-13
4	Fourier Transform of Data in Figure 3	2-15
5	Axial Electric Field Near Beam in Antisymmetric, Unmodified CCTWT	2-16
6	Fourier Transform of Data in Figure 5	2-17
7	Axial Electric Field Driven by Sinewave at Resonance	2-19
8	Axial Electric Field Driven by Sinewave off Resonance	2-21
9	Transverse Electric Fields in Cavity of Symmetric CCTWT	2-22
10	Transverse Magnetic Fields in Cavity of Symmetric CCTWT	2-23
11	Transverse Electric Fields in Cavity of Antisymmetric CCTWT	2-24
12	Transverse Magnetic Fields in Cavity of Antisymmetric CCTWT	2-25
13	Axial Electric Fields in Two Cavities of Symmetric CCTWT	2-26
14	Fourier Transform from Symmetric CCTWT with Membrane Dampers	2-28
15	Fourier Transform from Antisymmetric CCTWT with Membrane Dampers	2-29
16	Generated Geometries in SOS	3-4

LIST OF TABLES

TABLE		PAGE
1	Simulation Series for the CCTWT Coldtest	2-12
2	Resonant Frequencies in CCTWT Simulations	2-18

SECTION 1

INTRODUCTION

1.1 BACKGROUND

A vital step in the design of microwave power tubes is the "cold-test" (testing without an electron beam present) of the RF circuit or selected components thereof. The RF interaction circuit must satisfy the frequency and impedance requirements of the design, and for some tubes the phase, loss, and matching characteristics must also meet some requirements. For sufficiently accurate design analysis and optimization, some or all of these characteristics must be determined for each circuit to be analyzed. If some of these parameters are altered in the model in the course of meeting the design requirements, coldtest on actual circuits must be performed to determine what modifications are required to achieve the desired characteristics. Coldtest on actual circuits requires expensive and time-consuming machining and assembly, and the availability of expensive microwave-measurement equipment. Special "ports" or holes for measurement probes or field perturbers may be necessary for determining the characteristics of higher (or lower) modes which might cause problems (such as instabilities). Such modes may be very difficult to identify (as to field characteristics) by actual coldtest. Thus the availability of effective and economical, user-friendly codes to perform the tasks of coldtest would be highly advantageous. A number of useful codes exist for particular types of coldtest analysis in two-dimensions; however, many circuits of interest have little or no symmetry and so require a full three-dimensional analysis. Some attempts have been made to apply large three-dimensional electromagnetic and particle simulation codes to particular microwave tube problems (References 1 and 2); these have achieved varying but notable degrees of success. It is clear that a computer program (or programs) written specifically for the coldtest analysis of microwave tube circuits in three dimensions is required if the needs of the microwave tube industry is to be met.

1.2 DESCRIPTION OF THE PROGRAM

In response to this requirement, the Naval Research Laboratory has initiated the Program for Advanced Computational Techniques for Power Tube Design. The objective of the Program is to investigate and develop computational methods relevant to the coldtest of microwave power tubes, and to implement and integrate such methods into codes for effectively performing that function of the design process. The undertaking is an ambitious one. Numerical methods must be found or developed which are capable of solving Maxwell's equations in complex, three-dimensional geometries and with sufficient computational efficiency to allow use in a parametric sense. Equally important and challenging is the requirement that resulting codes be useful to design engineers, who are not specialists in computational physics.

The Program consists of three phases. In Phase 1 (Investigation), available computational methods for coldtest simulation will be assessed and a detailed plan developed. Actual code development will occur under Phase 2. Finally, in Phase 3, the software will be implemented and integrated by the manufacturer. Modifications and documentation will be produced by the software designer in response to the manufacturer's experience.

1.3 PHASE 1 SUMMARY

Mission Research Corporation (MRC) and Varian Associates, Inc., (VAI) have formed a team to participate in the NRL Program. This report is intended to document the experience and results of this team effort under Phase 1. This effort has been directed primarily at two related areas: (1) application of existing three-dimensional techniques to simulate coldtest of a circuit and (2) design of algorithms and software to be developed in Phases 2 and 3.

Section 2 of this report documents results of three-dimensional simulations of coldtest on a coupled cavity travelling wave tube (CCTWT) circuit. This work is an extension of our previous CCTWT simulations using a beam (References 2 and 3). For the present work, a sub-grid model was developed to accurately simulate the effects of stub and loop cable drives. By applying these to the CCTWT model, the symmetric and antisymmetric responses were obtained. Fourier transform results (using triangular pulse drive) were verified at specific frequencies. Attempts were then made to reduce the unwanted antisymmetric response by modifying the circuit, first by reducing the beam tunnel diameter and next by inserting resistive material at selected locations in the circuit. The latter approach proved successful; thus, we have demonstrated use of simulation methods to improve circuit design.

Section 3 of this report describes our recommended approach to the software development and implementation efforts in Phases 2 and 3. This is a result of our investigation of available methods, experience with actual coldtest simulations (see Section 2), and assessment of user requirements. Varian has produced a user requirements document (Reference 4) which encompasses the significant needs of the community. We believe that we should attempt, in Phases 2 and 3, to address both three-dimensional algorithm and computer-aided design issues, subject to resource constraints. Our approach and plan is based upon that premise.

SECTION 2

COLDTEST SIMULATION OF CCTWT

The simulations of a coupled-cavity, travelling wave tube (CCTWT) described herein are a continuation of previous work described in the report MRC/WDC-R-098, "Numerical Simulations of a Monotron Oscillator Cavity and a Coupled-Cavity Travelling Wave Tube." That work led to an IEEE report, "Transient Analysis of Beam Interaction with Antisymmetric Mode in Truncated Periodic Structure Using 3-Dimensional Computer Code "SOS"." The recent simulations were part of an effort to find out how to reduce an undesired, antisymmetric, resonant mode in the CCTWT without reducing the desired, symmetric mode. Our approach was to use the SOS code to simulate a coldtest of a section of the CCTWT, observe the behavior of the electromagnetic fields, deduce from those observations some modifications to CCTWT, and then test the modifications by simulating them with SOS.

2.1 DESCRIPTION OF THE SOS CODE

SOS is a three-dimensional, fully dynamic and self-consistent particle-in-cell (PIC) code used to simulate plasma physics problems. The name of the code is derived from the Self-Optimized-Sector technique it employs to efficiently handle the immense data management problem posed by a typical simulation. This technique allows the treatment of problems involving millions of data cells and particles instead of the mere tens of thousands permitted by other codes. In SOS, the time-dependent Maxwell equations are solved in finite-difference to obtain electromagnetic fields. The plasma is represented using macroparticles, with trajectories obtained relativistically from the full Lorentz force. The particle ensemble forms a current density for the Maxwell equation; thus, the method is self-consistent.

SOS offers a large number of algorithms and options within a single code. For example, there are two coordinate systems available (Cartesian and cylindrical), and a two-dimensional Poisson solution is available to generate TEM waveforms. The particle creation algorithm allows field-, photo-, and beam emission processes. A unique capability exists in the geometry generator for non-conformal generic shapes (cylinders, cones, etc.) and in the sub-grid modeling algorithms, which allow quasi-static treatment of structural details on scales much smaller than can be resolved by the spatial mesh. Examples of the latter include fine structured capacitive, inductive, and resistive effects.

The SOS code also offers interactive capability through the Interactive Front End (IFE). The IFE allows the user to create an input data file while simultaneously receiving HELP (data sequence and variable definitions, modeling information), on-line graphics to depict structural details, on-line error diagnostics, and the ability to recall, change, and save information. The IFE is basically an editor, and functions either in a prompt model or an unstructured mode.

SOS was initially developed by MRC personnel under contract to the Air Force Weapons Laboratory (AFWL) for use in system-generated electromagnetic pulse (SGEMP) research. Since then, the code has been adopted for use at Sandia National Laboratories (SNLA) to model magnetically insulated power transmission and charged particle beam physics. The SOS code is operational in the same version on both VAX-11/780 and Cray-1 computers.

2.2 SUB-GRID MODEL OF COLD-TEST CABLE

2.2.1 Objective

Cold-test of a circuit is commonly performed by introducing rf signal through a coaxial cable. The cable penetrates the cavity wall to the

interior, and terminates in either an open circuit (stub) or a short circuit (loop). To simulate this experimental technique, we have developed a model which will duplicate the radiation effect, even though cable dimensions are typically much smaller than the available spatial grid. It is typical of the group of models commonly referred to as "sub-grid" models. The principal feature of this model is that it preserves the exact theoretical relationship between the strength of the incident cable current and that of the resulting electromagnetic fields. However, the model cannot be driven by the cavity, and therefore has no effect on the "Q" of the system. This deficiency may be remedied in future versions.

2.2.2 Standing Wave Solutions

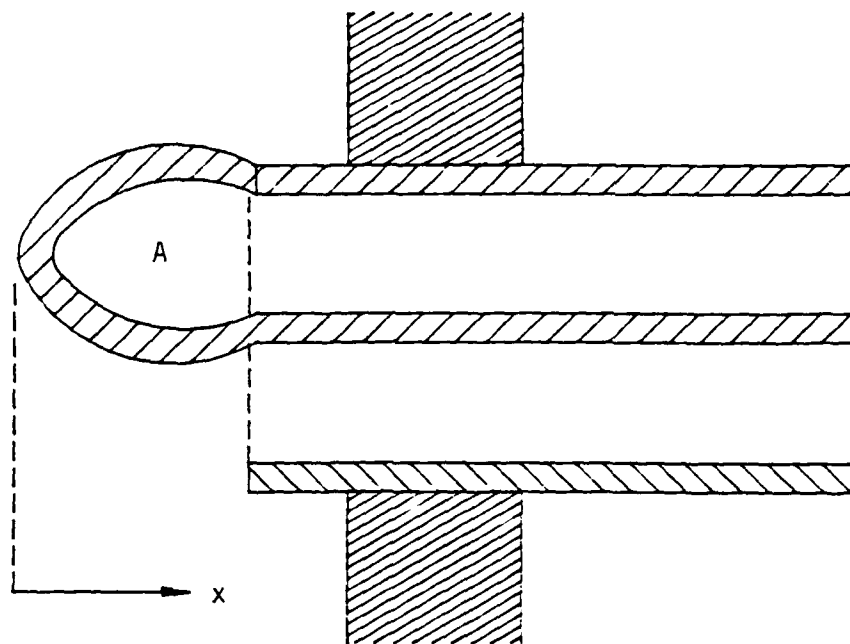
First, we consider the travelling waves,

$$I^{\pm}(x,t) = \pm I_0^{\pm} \sin \omega(x/c \mp t) \quad (2-1)$$

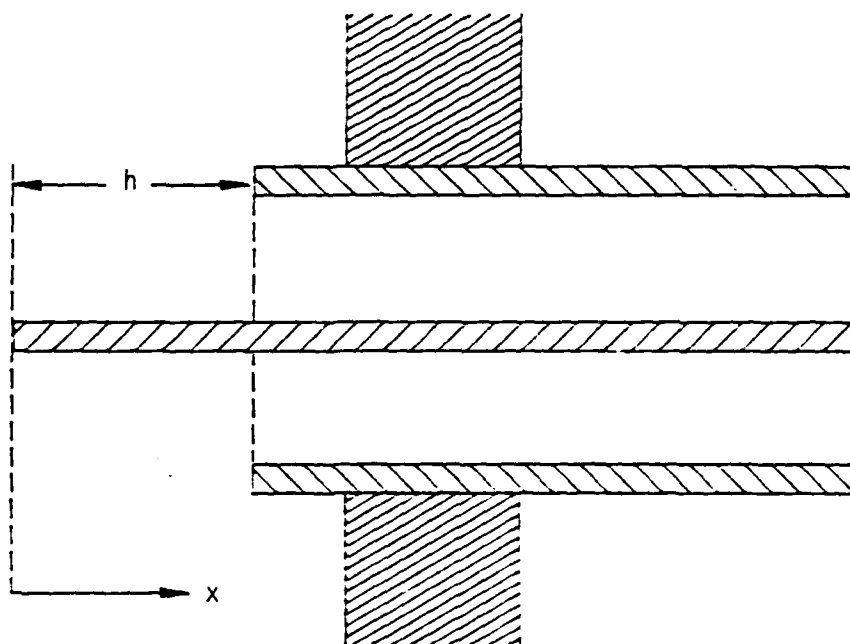
$$V^{\pm}(x,t) = \pm I_0^{\pm}/Z \sin \omega(x/c \mp t) ,$$

which represent transverse electromagnetic (TEM) waves in a coaxial cable. (The upper sign describes a wave travelling from left to right, and the lower from right to left.) The current and voltage magnitudes are related by the cable impedance, Z , and the phase velocity equals the speed of light in vacuum.

Next, consider the two types of termination illustrated in Figure 1. For the open-circuit termination (Figure 1a), the current at the origin ($x=0$) must vanish. Thus, an incident rf pulse from the right must be cancelled by a wave from the left. In terms of the travelling waves described in Equation (2-1), the boundary condition,



(b) Loop Cable Model



(a) Stub Cable Model

Figure 1. Geometry for Cable Models.

$$I_0^+ = + I_0^- , \quad (2-2)$$

results in the solution,

$$I(x,t) = + 2I_0^- \sin \omega x / c \cos \omega t \quad (2-3)$$

$$V(x,t) = - 2I_0^- / Z \cos \omega x / c \sin \omega t .$$

The stub length is assumed to be short compared to the wavelength, or

$$h \ll 2\pi c / \omega . \quad (2-4)$$

For the closed-circuit termination shown in Figure 1b, the boundary condition requires that the voltage at the origin vanish. Here, we are assuming that the loop dimensions are small compared to the wavelength, so that resonance effects may be neglected. This boundary condition,

$$I_0^+ = - I_0^- , \quad (2-5)$$

yields the solution,

$$I(x,t) = + 2I_0^- \cos \omega x / c \sin \omega t \quad (2-6)$$

$$V(x,t) = - 2I_0^- / Z \sin \omega x / c \cos \omega t .$$

Thus, both terminations produce simple standing wave solutions, subject to the constraint in Equation (2-4).

2.2.3 Sub-Grid Models

Beginning with the open-circuit termination, we write an expression for the dipole moment,

$$p = \int_0^h dx \, x \, \rho . \quad (2-7)$$

Then the time derivative of the dipole moment is

$$\partial_t p = \int_0^h dx \, x \, \partial_t \rho . \quad (2-8)$$

From the one-dimensional continuity equation,

$$\partial_t \rho + \partial_x I = 0 , \quad (2-9)$$

this becomes

$$\partial_t p = - \int_0^h dx \, x \, \partial_x I . \quad (2-10)$$

Integration by parts yields the simpler form,

$$\partial_t p = - x I \Big|_0^h + \int_0^h dx \, I . \quad (2-11)$$

Next, use is made of the standing wave solution in Equation (2-3). Due to the constraint in Equation (2-4), we can approximate the stub current as

$$I(x,t) = + 2I_0^- \omega x/c \cos \omega t . \quad (2-12)$$

Substitution of the approximate current into Equation (2-11) yields the result,

$$\partial_t p = 2I_0^- (\omega h^2/2c) \cos \omega t . \quad (2-13)$$

This result can be applied to any dynamic electromagnetic algorithm through a corrective term,

$$E^{k+1} = (E^{k+1})_a - \frac{\delta t}{\epsilon_0 \delta x \delta y \delta z} \partial_t p, \quad (2-14)$$

or

$$E^{k+1} = (E^{k+1})_a - \frac{\delta t \omega h^2 2I_0^-}{2\epsilon_0 c \delta x \delta y \delta z} \cos \omega t. \quad (2-15)$$

This applies to a single component of electric field in a Cartesian coordinate system with cell dimensions, δx , δy , and δz . The superscript, k , denotes time and the subscript, a , stands for standard algorithm results, i.e., contributions from curl of the magnetic field and current density due to free charge.

The sub-grid model for the closed-circuit termination is obtained by analogy with the derivation of dipole moment. That is, we define a magnetic moment,

$$\bar{m} = \int dx^3 \bar{r} \times \bar{J}, \quad (2-16)$$

or

$$m = -IA \quad (2-17)$$

with respect to Figure 1b. Again making use of the restriction of Equation (2.4), the current in Equation (2-6) is given approximately by

$$I(x,t) = + 2I_0^- \sin \omega t \quad (2-18)$$

Then the time derivative of the magnetic dipole is

$$\partial_t m = - 2I_0^- \omega A \cos \omega t \quad (2-19)$$

The correction to the dynamic magnetic field is

$$B^{k+3/2} = (B^{k+3/2})_a - \frac{\delta t \mu_o}{\delta x \delta y \delta z} a_t^m, \quad (2-20)$$

or

$$B^{k+3/2} = (B^{k+3/2})_a + \frac{\delta t \mu_o \omega A 2I_o^-}{\delta x \delta y \delta z} \cos \omega t. \quad (2-21)$$

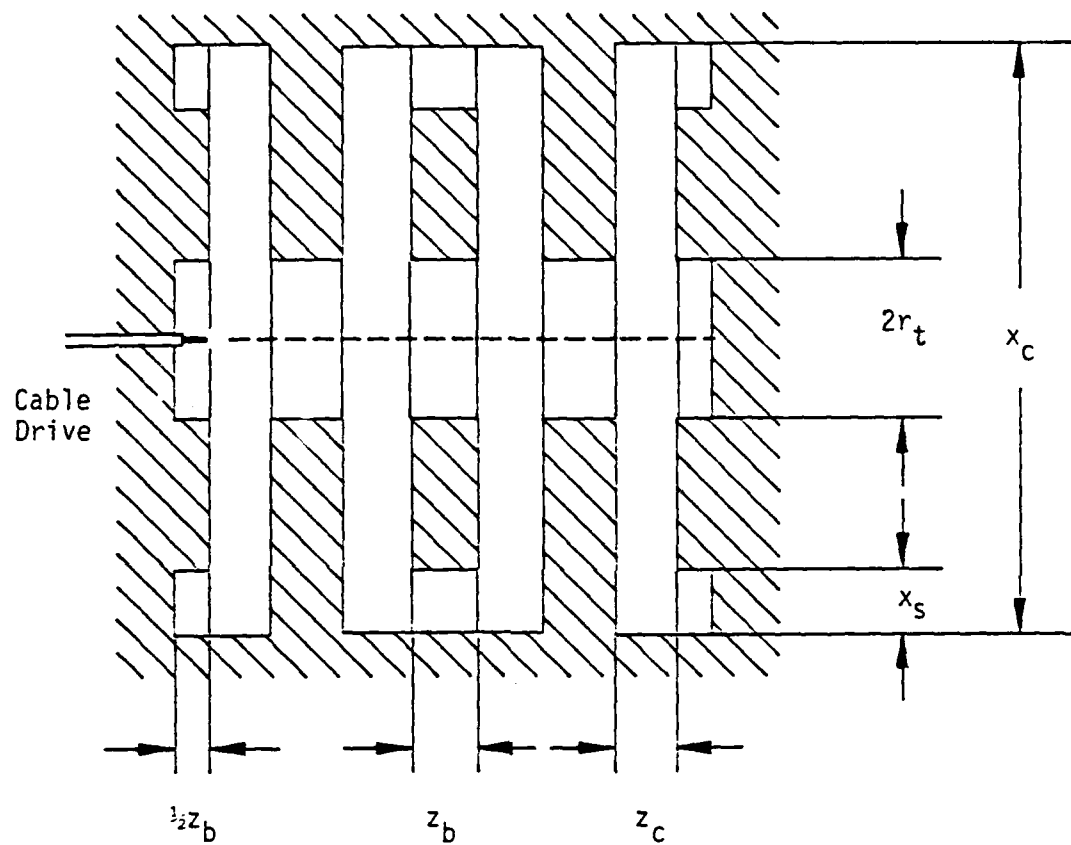
Here the standard algorithm result (subscript, a) contains only contributions from the curl of the electric field.

Note that in both the stub cable model (Equation (2-15)) and the loop cable model (Equation 2-21)), the current ($2I_o^-$) represents the peak of the standing wave.

2.3 MODEL OF THE CCTWT

The simulation model was a lossless, resonated section of a coupled-cavity travelling wave tube (CCTWT). The cavities were square in cross-section, and the coupling slots (two per barrier plate) alternated in orientation between vertical and horizontal planes. The beam tunnel was centrally located cylinder connecting the square cavities. This simulation problem is inherently three-dimensional and thus a natural candidate for analysis using the SOS code (Reference 5).

The basic geometry and spatial dimensions for the CCTWT Model are shown in Figure 2. This is a view from the top of the tube which indicates the four cavities, the centrally located beam tunnel, and the pairs of vertical coupling slots through the barrier plates. The cavity depth (along the beam axis) and the barrier plate thickness were identical at 0.422 inches.



$$\begin{aligned} z_b &= 0.422 \text{ in} \\ z_c &= 0.422 \text{ in} \\ r_t &= 0.375 \text{ in} \\ x_s &= 0.312 \text{ in} \\ x_c &= 2.060 \text{ in} \end{aligned}$$

Figure 2. CCTWT Model Geometry and Dimensions.

This basically rectangular geometry is well suited to the Cartesian coordinates option in SOS, although "stepping" was required to model the beam tunnel. Use was made of two planes of mirror symmetry intersecting at the beam axis to reduce computational costs by a factor of four. With these symmetries, a side view of the actual computer model is shown in Figure 11, which may be compared with Figure 10. (Figure 10 shows the vertical coupling slots, and Figure 11 the horizontal.) Figure 12 is an end view of a barrier plate, which illustrates the stepped beam tunnel, the two planes of mirror symmetry, and a horizontal coupling slot. The spatial grid is observed to be approximately square, but varies slightly in the x and y coordinates to exactly match the tube dimensions while preserving x-y spacing symmetry. The spacing was approximately 2×10^{-3} m, which will support frequencies up to about 25 GHz. A time step of 4 psec was used with typical total simulation times of 4 nsec. Note that the number of spatial cells in this model is only 5,408 ($13 \times 13 \times 32$). By contrast, simulations with SOS on other problems have typically required several hundred thousand cells. Therefore, the present simulation is relatively modest, and the crudeness of the model could easily be refined to improve accuracy of the results.

Using mirror symmetry boundaries allows only symmetric electromagnetic modes to exist in the simulation. To observe only antisymmetric modes, one of the boundaries was replaced by a perfectly conducting plane, which serves as an antisymmetric mirror symmetry boundary. At such a plane, the components of the reflected electric field parallel to the plane are reversed in direction, while the normal component remains unchanged; on the plane, only the normal component of electric field exists, which is what is expected of a conductor. Analyzing both modes required separate runs of SOS with both types of boundaries.

To coldtest the CCTWT, the cable driver sub-grid model was used to excite electromagnetic modes within the cavities. The driver was placed at cell (1,1,1), which is the center of the hole where the electron beam would enter the first cavity. To excite symmetric modes, a stub driver with a stub length of 0.5 mm was used, producing an axially oriented electric dipole field. To excite antisymmetric modes, a loop driver with a loop area of 0.25 mm² was used, producing a vertically oriented magnetic field.

The simulation output capability of SOS includes time histories and vector plots. Time histories of any component of the electromagnetic field at any location in the spatial grid may be plotted for the duration of the simulation. Also, Fourier transforms of these time histories may be plotted to determine the resonant frequencies of different electromagnetic modes. Vector plots present a two-dimensional array of arrows representing electric or magnetic fields in any plane within the spatial grid. These plots show the spatial variations of electromagnetic fields so that resonant mode can be identified.

2.4 CALCULATED RESULTS

Table 1 summarizes ten of the nineteen simulations made in trying to understand the CCTWT and suppress the undesired, antisymmetric mode. Runs 6 and 7 showed the frequencies of modes in an unmodified CCTWT, while runs 8 and 10 focused on two particular modes. Runs 12 and 13 show the effects of shrinking the beam hole in the barrier plates. Runs 14 and 15 supplement information gained in runs 6 and 7, and runs 18 and 19 show the effects of adding membrane dampers to the slots in the barrier plates.

The first step in suppressing the undesired antisymmetric mode was to get an indication of the various modes present in the CCTWT. To this end, both symmetric and antisymmetric simulations were driven with a single, 200 ps-wide, triangular pulse, exciting a wide range of frequencies. Figure 3 shows the time history of axial component of electric field near the axis

TABLE 1
SIMULATION SERIES FOR THE
CCTWT COLDTEST

<u>Run</u>	<u>Symmetry</u>	<u>Driver</u>	<u>Excitation</u>	<u>Comment</u>
CCTWT86-6	Symm.	Stub	200 ps triangle	FFT plots of unmodified, symmetric CCTWT
CCTWT86-7	Anti.	Loop	200 ps triangle	FFT plots of unmodified, antisymmetric CCTWT
CCTWT86-8	Symm.	Stub	3.76 GHz sine	Vector plots of a symmetric mode
CCTWT86-10	Anti.	Loop	5.45 GHz sine	Vector plots of antisymmetric mode
CCTWT86-14	Symm.	Stub	200 ps triangle	Supplemental time histories for CCTWT86-6
CCTWT86-15	Anti.	Loop	200 ps triangle	Supplemental time histories for CCTWT86-6
CCTWT86-18	Anti.	Loop	200 ps triangle	Effect of membrane damper on FFT's
CCTWT86-19	Symm.	Stub	200 ps triangle	Effect of membrane damper on FFT's

SOS VERSION: JANUARY 1986 DATE: 3-JUN-86
SIMULATION: CCTWT86-14

TIME HISTORY PLOT
E3 COMPONENT
AT COORDINATE (5,1,21)

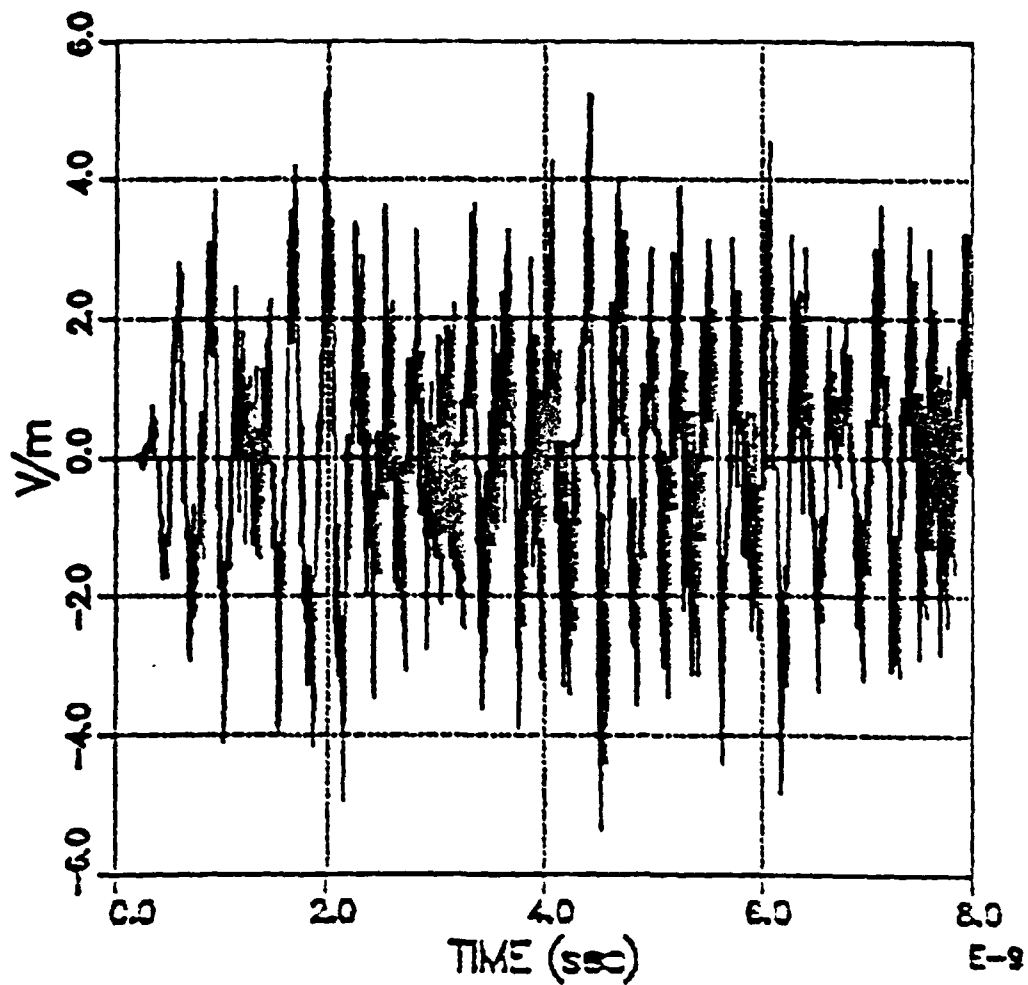


Figure 3. Axial Electric Field Near Beam in Symmetric, Unmodified CCTWT

in the symmetric simulation, corresponding to the edge of the electron beam in the actual device. The axial electric field at this location modulates the beam current, which in turn may amplify this signal and reinforce the electromagnetic mode that gave rise to it. Figure 4 shows a Fourier transform of the same data for frequencies from 0.5 GHz to 10.0 GHz. Figures 5 and 6 show the axial electric field and Fourier transform for the same location in the antisymmetric case.

Table 2 lists the major frequency peaks below 8 GHz observed in the Fourier transforms produced by these runs, and it also compares them to frequency peaks observed in previous runs of an eight-cavity CCTWT driven by an electron beam.

The frequencies observed in the later simulations resemble those observed in the earlier simulations, suggesting that beam loading had little effect on these frequencies. The range of frequencies from 2 GHz to 4 GHz, present in the symmetric simulations, forms a lower passband which is believed to be a viable operating region for the CCTWT. The peak at 3.7 GHz is the strongest peak in Figure 4, so it was singled out as a representative symmetric mode. The lack of frequencies above 3.7 GHz in the beam-driven, symmetric case is the result of turning on beam with a smooth ramp function designed to suppress high frequency components. The cable drive function is quite sharp by comparison and excites many high-frequency modes. The lack of a 3.8 GHz peak in the cable-driven, antisymmetric case is probably the result of using four cavities instead of eight cavities to model the CCTWT, as was done in the beam-driven case. Consequently, the peaks near 5.4 GHz were given the most attention in preceeding, antisymmetric simulations.

Driving a lossless cavity at resonance should produce linear growth of the electromagnetic fields associated with a particular mode. Figure 7 shows the growth of the axial component of electric field in the third cavity from the beam inlet. This was taken from a symmetric simulation excited by a 3.7 GHz sine wave. The growth is roughly linear,

SOS VERSION: JANUARY 1985 DATE: 3-JUN-86
SIMULATION: CCTWT86-14

TIME HISTORY PLOT
MAGNITUDE OF FFT OF E3 COMPONENT
AT COORDINATE (5,1,21)

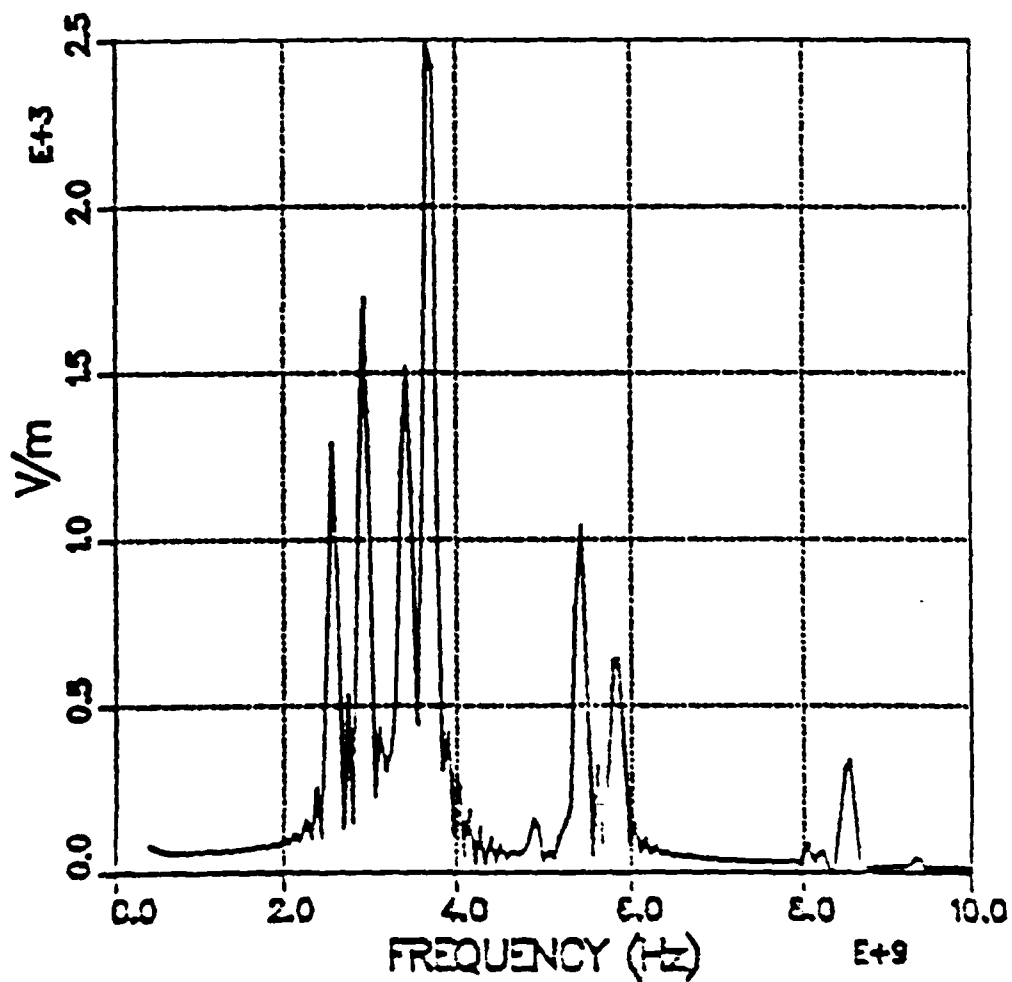


Figure 4. Fourier Transform of Data in Figure 3

SOS VERSION: JANUARY 1986 DATE: 3-JUN-85
SIMULATION: CCTWT86-15

TIME HISTORY PLOT
E3 COMPONENT
AT COORDINATE (5,1,21)

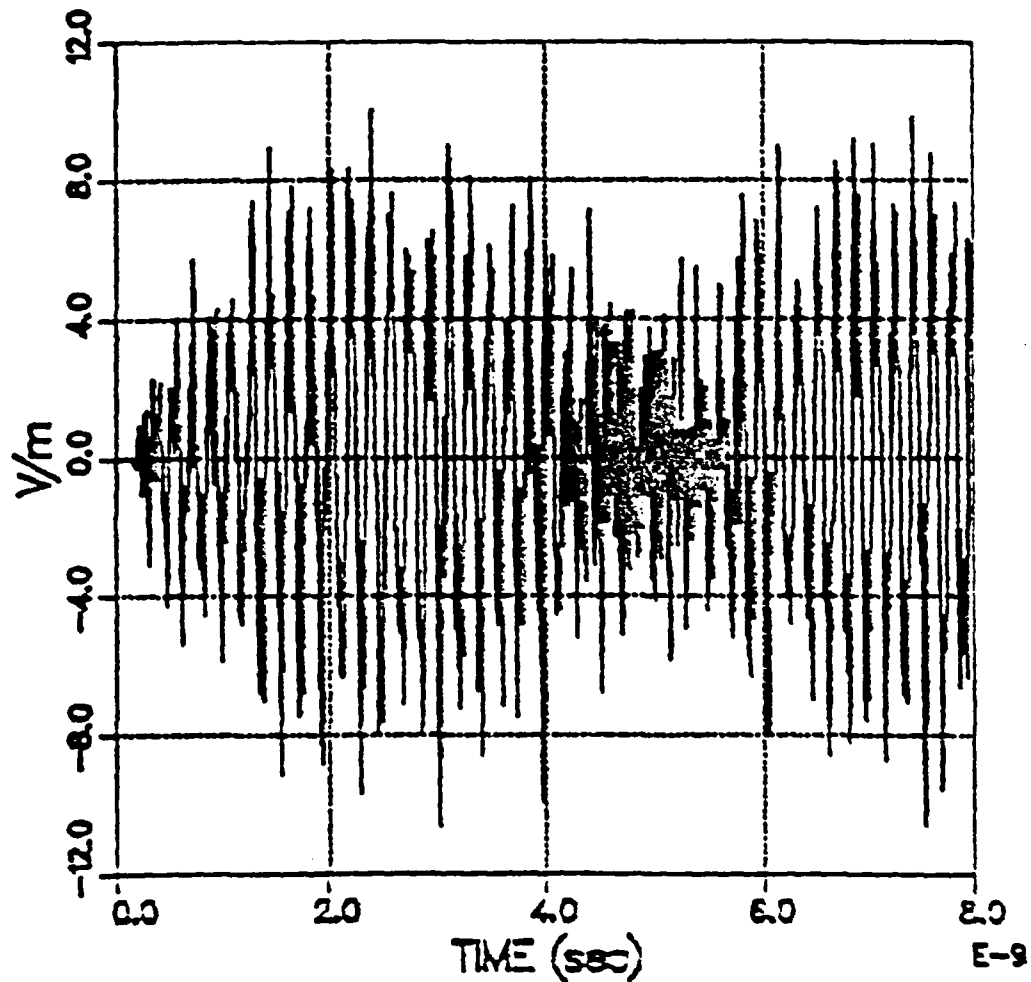


Figure 5. Axial Electric Field Near Beam in Antisymmetric, Unmodified CCTWT

SOS VERSION: JANUARY 1986 DATE: 3-JUN-85
SIMULATION: CCTKT86-15

TIME HISTORY PLOT
MAGNITUDE OF FFT OF E3 COMPONENT
AT COORDINATE (5,1,21)

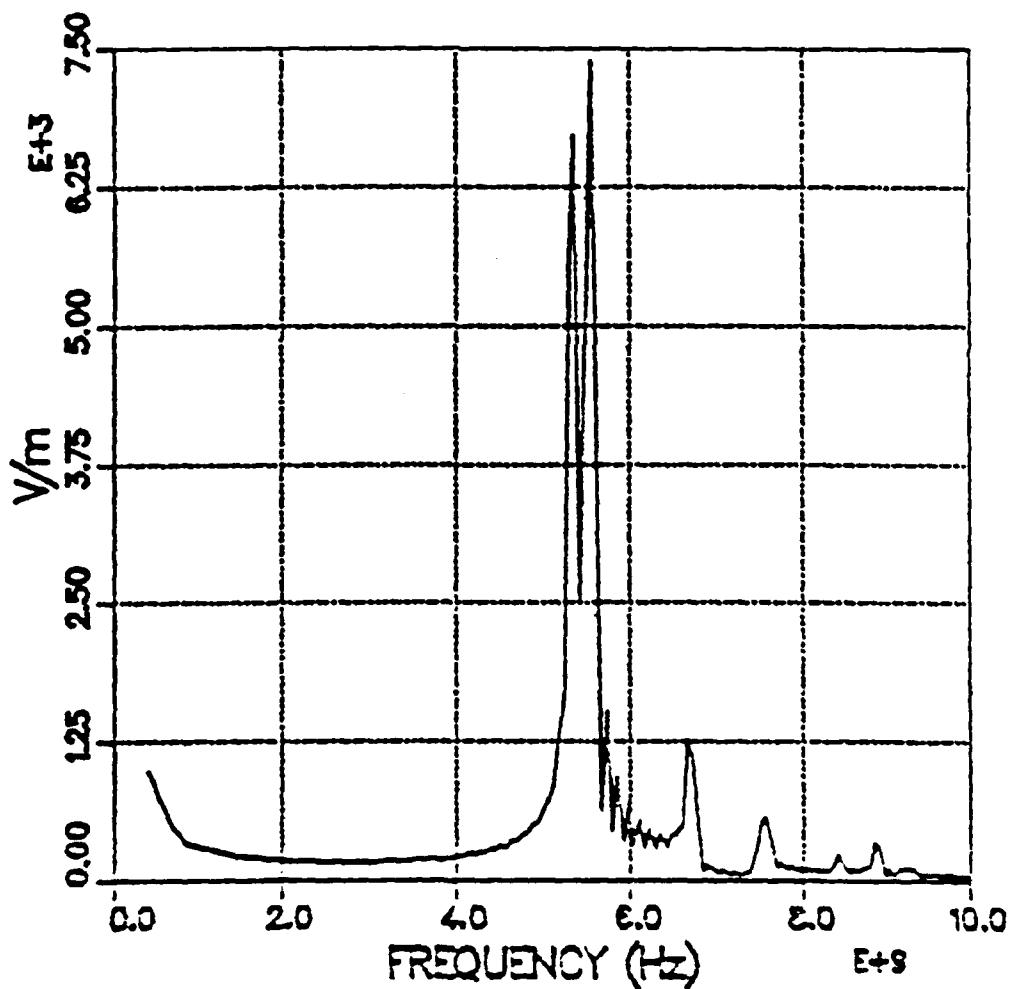


Figure 6. Fourier Transform of Data in Figure 5

TABLE 2
 RESONANT FREQUENCIES IN CCTWT SIMULATIONS

<u>Symmetric</u>		<u>Antisymmetric</u>	
Beam	Cable	Beam	Cable
<u>CCTWT-3</u>	<u>CCTWT86-6</u>	<u>CCTWT-5</u>	<u>CCTWT86-7</u>
2.4			
2.5			
	2.6		
	2.9		
	3.4		
3.5			
3.7	3.7		
		3.8	
	4.9		
		5.3	5.3
	5.4	5.4	5.4
		5.5	5.5
	5.8		
		6.6	
			6.7
		7.5	7.5

SOS VERSION: JANUARY 1986 DATE: 28-MAY-85
SIMULATION: CCTWT85-8

TIME HISTORY PLOT
E3 COMPONENT
AT COORDINATE (8,1,21)

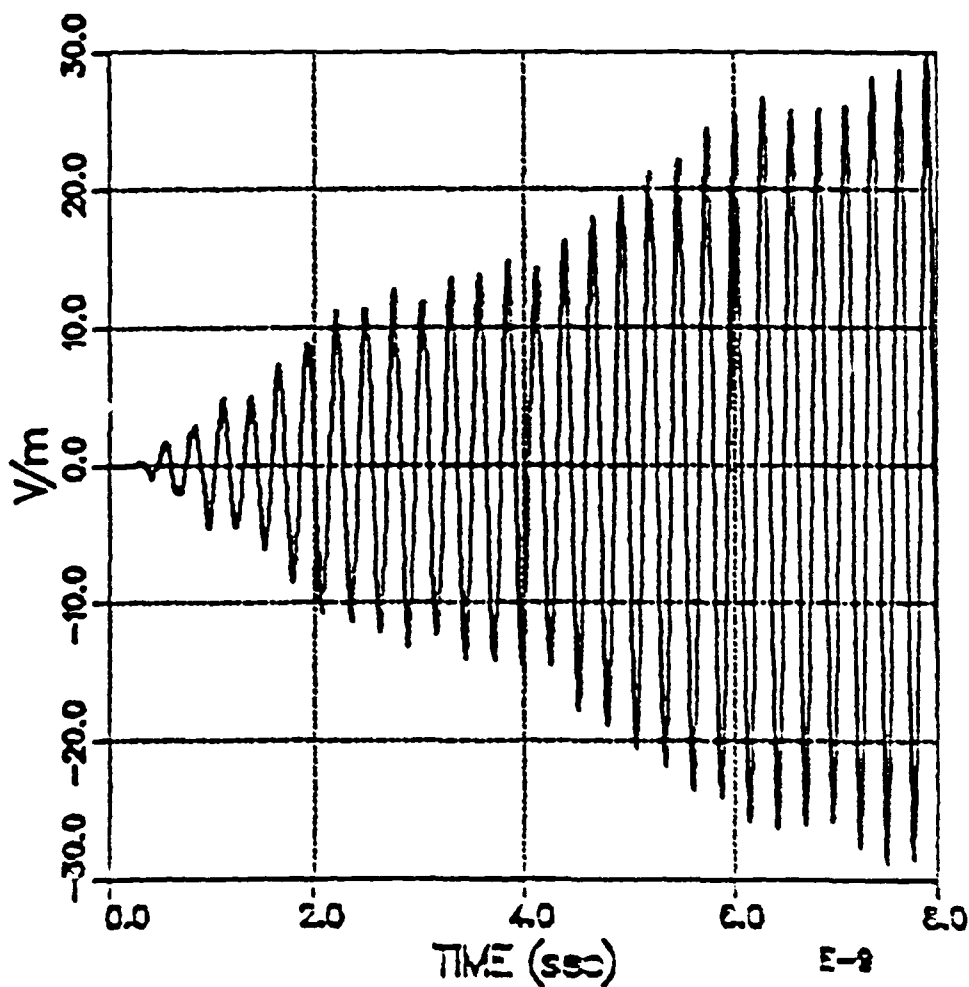


Figure 7. Axial Electric Field Driven by Sinewave at Resonance

but the envelope oscillates slightly because of another resonant mode at 3.4 GHz. Figure 8 shows the same axial field but from an antisymmetric simulation driven at 5.45 GHz. This frequency is off resonance by about 0.1 GHz, which is evidenced by the envelop returning to zero at about 10 ns.

The 3.7 GHz symmetric mode has the transverse electric and magnetic fields shown in Figures 9 and 10. These fields existed midway between the barrier plates of the second cavity from the beam inlet at 7.88 ns into the simulation. Figures 11 and 12 show the fields in the same cavity for the antisymmetric simulation driven by a 5.45 GHz sine wave. The magnetic fields in Figures 10 and 12 correspond to the "1-H" and "2-H" modes described in the previous MRC report.

Figure 13 shows axial electric fields of the 3.7 GHz symmetric mode throughout the second and third cavities. The electric field is strongest in between the barrier plates, while the field in the slot and beam hole is relatively weak. This suggested that reducing the size of the beam hole would not much affect the desired, symmetric mode, while possibly attenuating the undesired, antisymmetric mode. However, further simulations with the beam hole radius reduced by 20% showed about equal attenuation of both modes, and so this modification is not useful for selectively attenuating the antisymmetric mode.

Comparing Figures 9 and 1, the electric field near the horizontal slot (the upper portion of both plots) was strong next to the symmetric boundary at $X1 = 0.0$ (left side of Figure 9), but was nearly zero next to the antisymmetric boundary (left side of Figure 11). A similar situation existed in the slots, so that on either side of the symmetry boundary, the antisymmetric mode concentrated its electric field toward the edge of the slot, while the symmetric mode peaked towards the center of the slot. This suggested that a resistive damper near the ends of the slots would attenuate the antisymmetric mode more than the symmetric mode. A pair of simulations, with dampers at the ends of all of the slots, showed this to be true.

SOS VERSION: JANUARY 1986 DATE: 28-MAY-86
SIMULATION: CCTWT86-10

TIME HISTORY PLOT
E3 COMPONENT
AT COORDINATE (8,1,21)

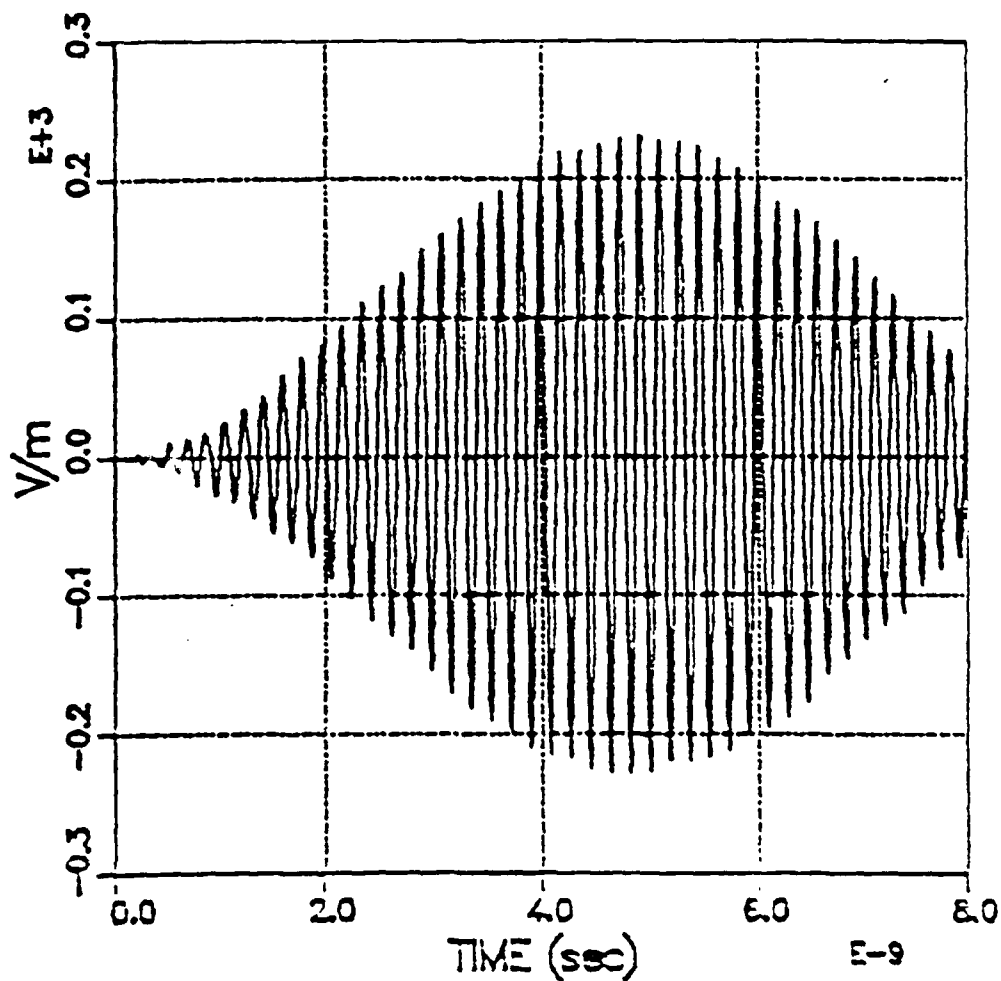


Figure 8. Axial Electric Field Driven by Sinewave off Resonance

SOS VERSION: JANUARY 1986 DATE: 28-MAY-85
SIMULATION: CCTWT86-8

VECTOR PLOT OF (E1,E2)
AT TIME: 7.88E-09 SEC
X3 = 3.22E-02 (m), VMAX = 3.60E+00

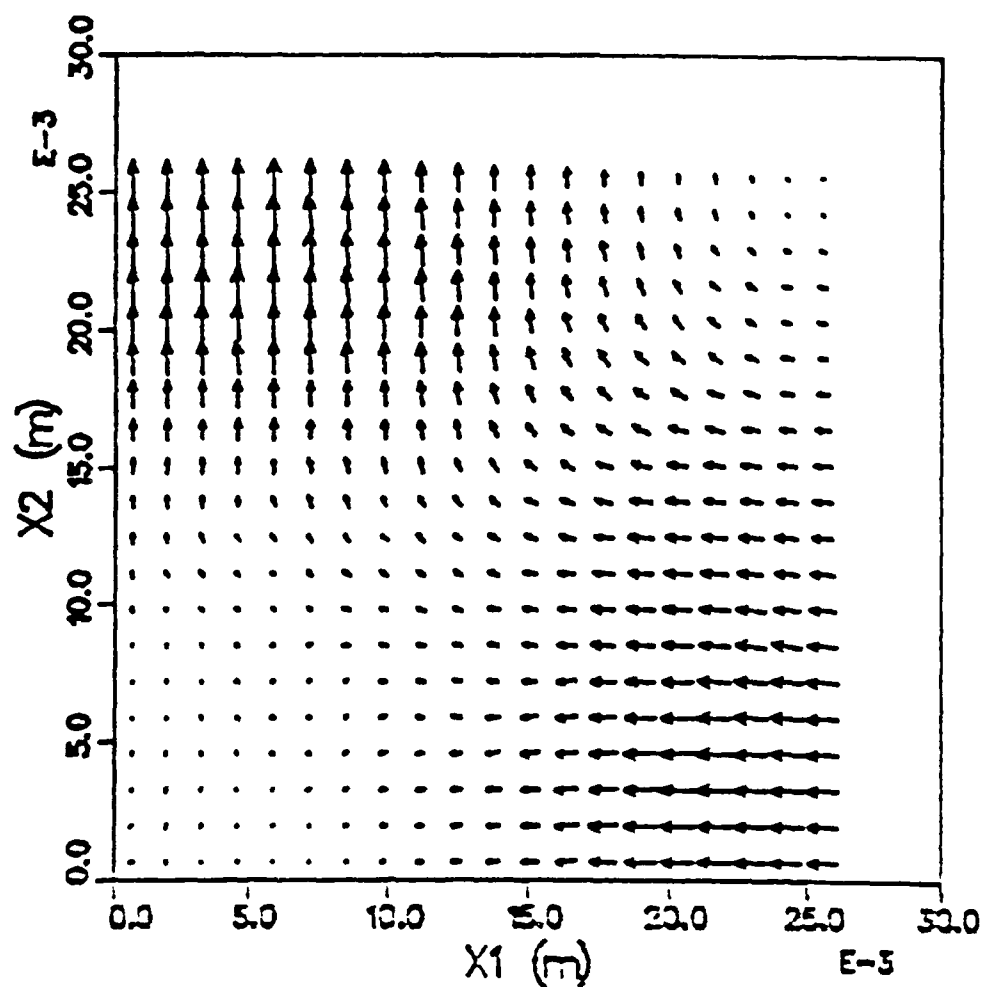


Figure 9. Transverse Electric Fields in Cavity of Symmetric CCTWT

SOS VERSION: JANUARY 1986 DATE: 28-MAY-86
SIMULATION: CCTWT86-8

VECTOR PLOT OF (B1,B2)
AT TIME: 7.89E-09 SEC
X3 = 3.22E-02 (m), VMAX = 8.41E-08

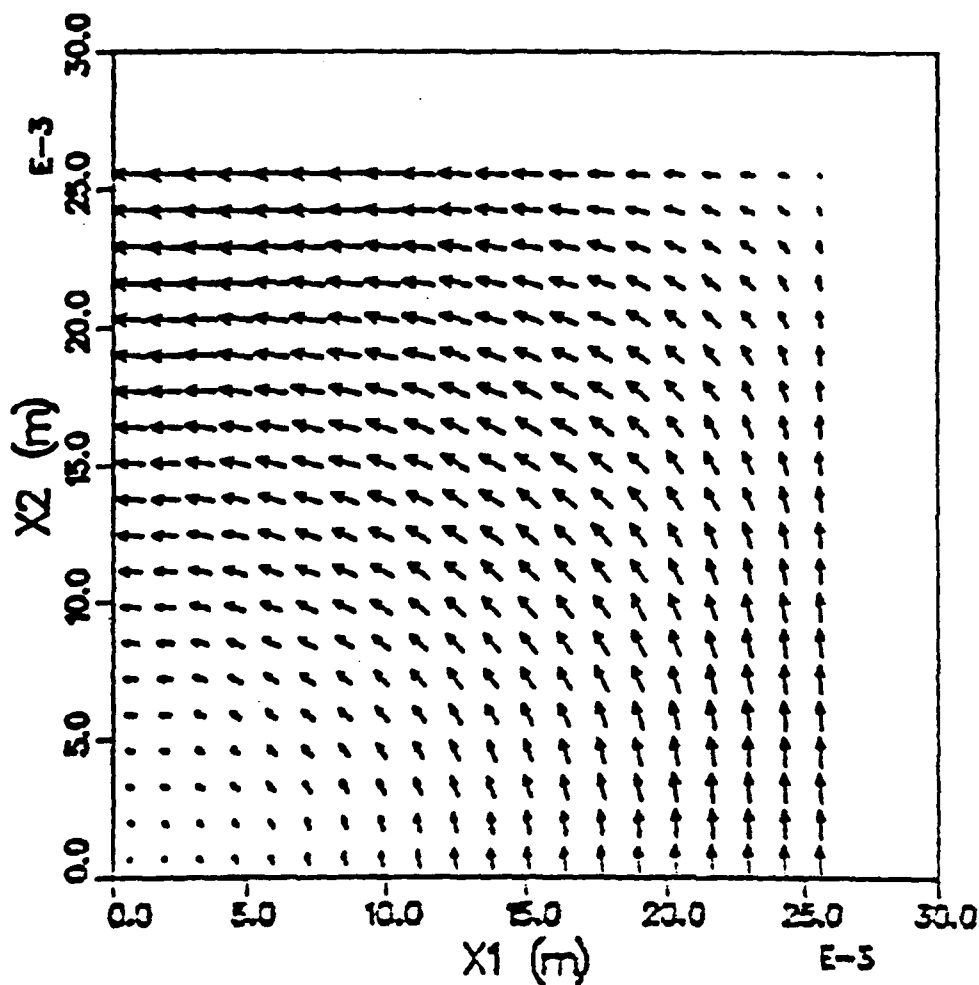


Figure 10. Transverse Magnetic Fields in Cavity of Symmetric CCTWT

SOS VERSION: JANUARY 1986 DATE: 28-MAY-86
SIMULATION: CCTWT86-10

VECTOR PLOT OF (E1,E2)
AT TIME: 7.88E-09 SEC
X3 = 3.22E-02 (m), VMAX = 2.77E+01

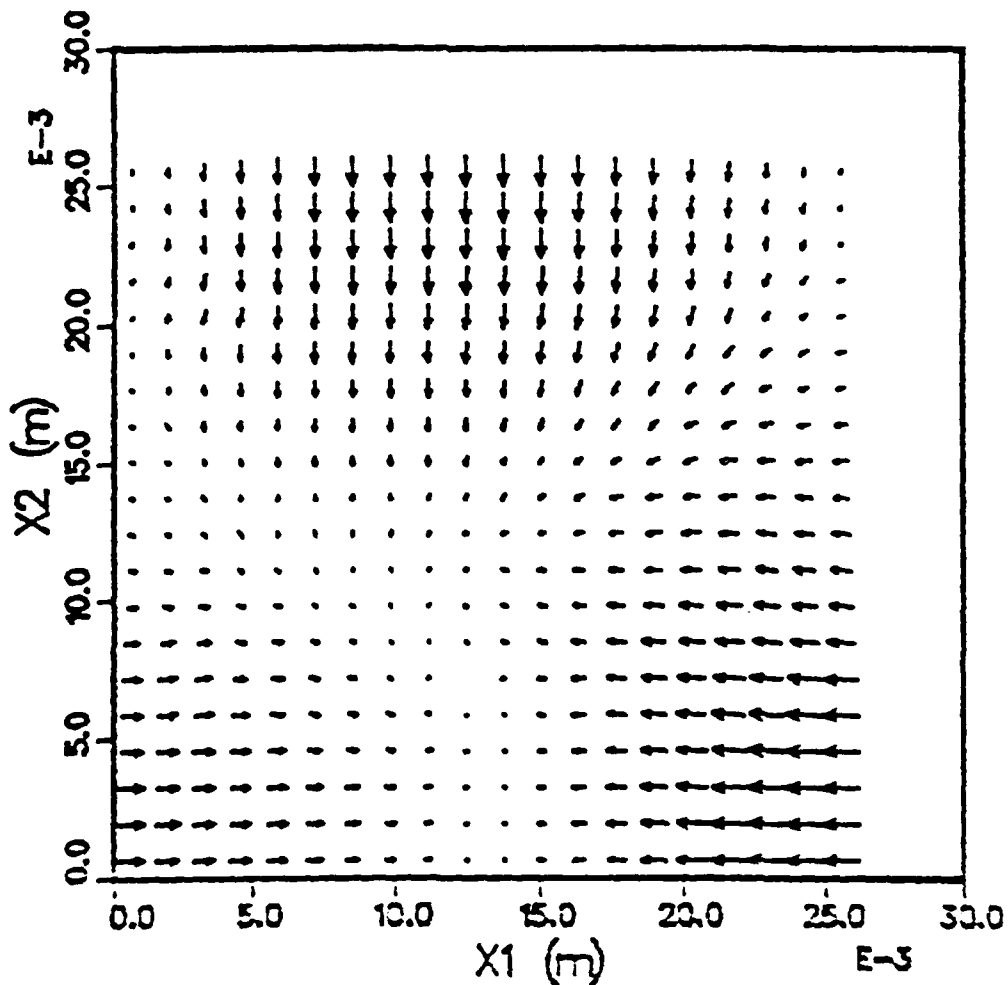


Figure 11. Transverse Electric Fields in Cavity of Antisymmetric CCTWT

SOS VERSION: JANUARY 1986 DATE: 28-MAY-86
SIMULATION: CCTWT86-10

VECTOR PLOT OF (B1,B2)
AT TIME: 7.88E-09 SEC
X3 = 3.22E-02 (m), VMAX = 2.33E-07

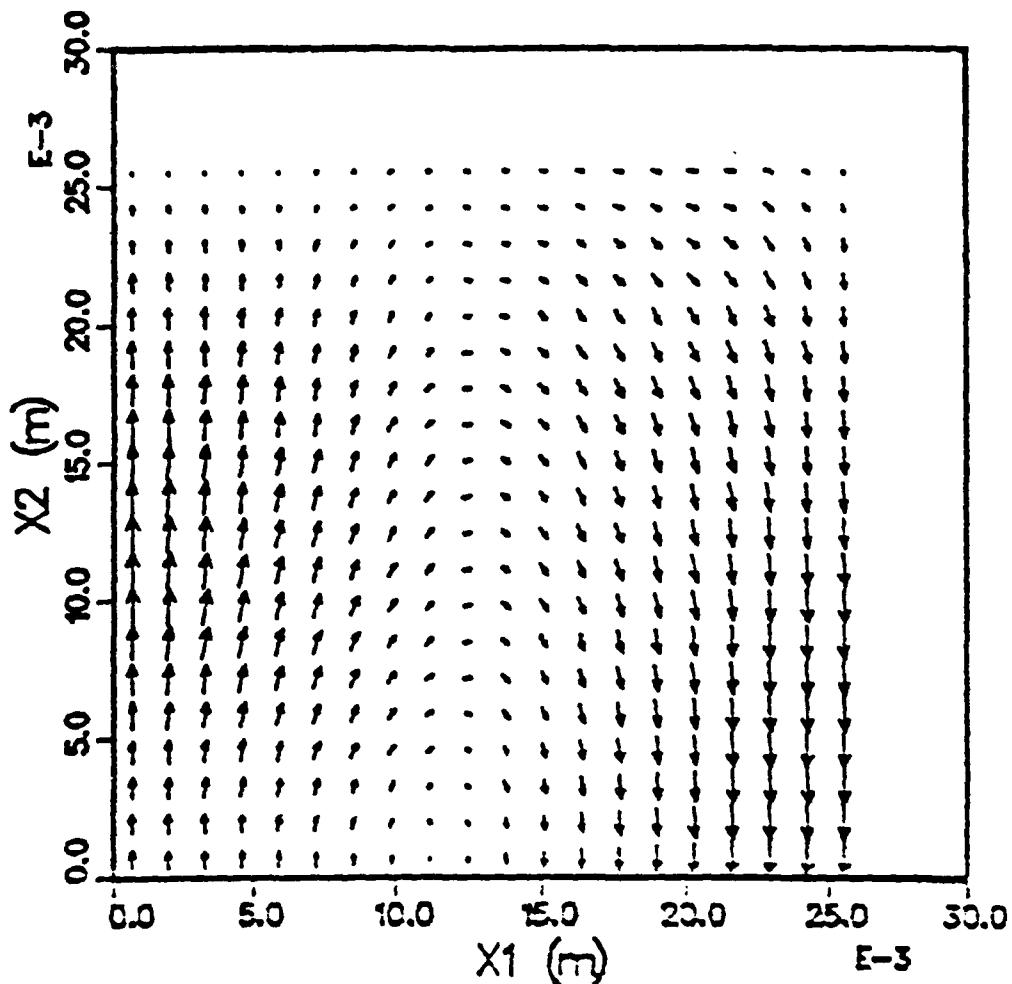


Figure 12. Transverse Magnetic Fields in Cavity of Antisymmetric CCTWT

SOS VERSION: JANUARY 1985 DATE: 28-MAY-85
SIMULATION: CCTWT86-8

VECTOR PLOT OF (E3,E1)
AT TIME: 7.88E-09 SEC
X2 = 0.00E+00 (m), VMAX = 2.93E+01

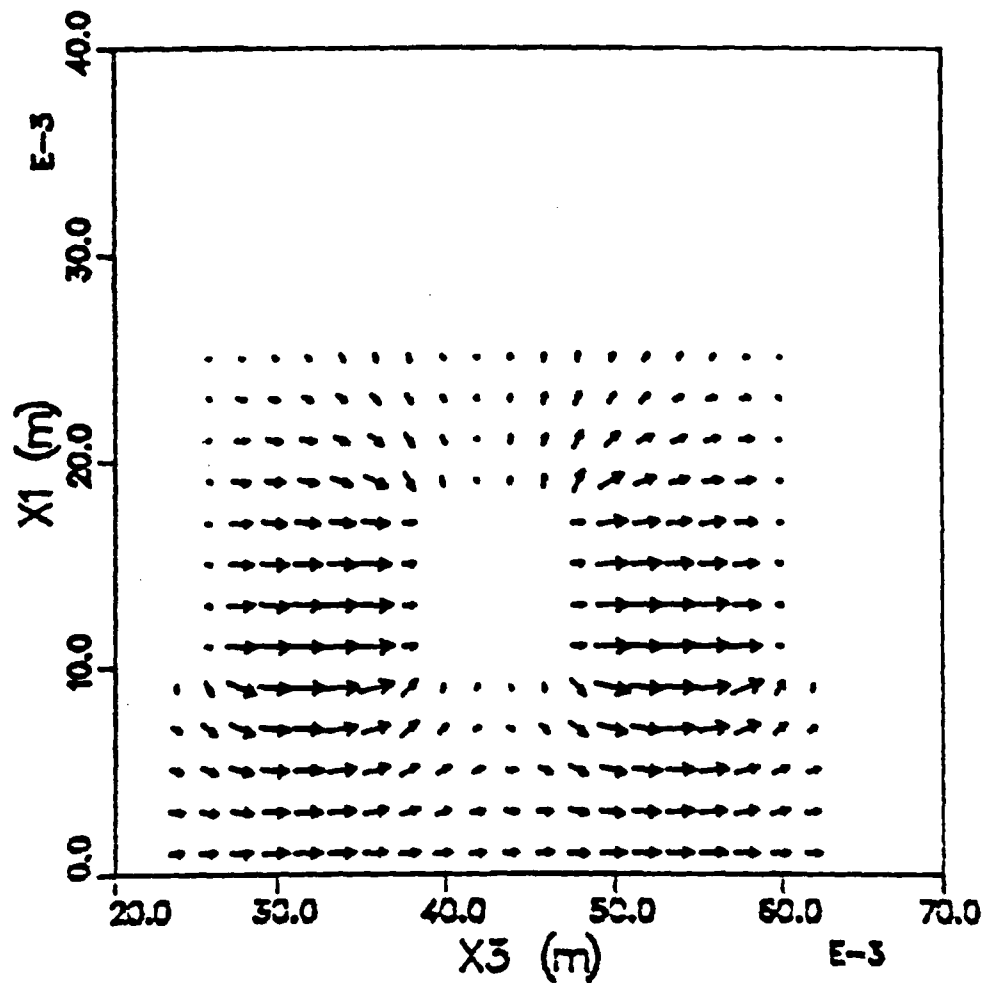


Figure 13. Axial Electric Fields in Two Cavities of Symmetric CCTWT

Figure 14 shows the Fourier transform of axial electric field comparable to Figure 4, the only difference being the presence of the dampers; the 3.7 GHz symmetric mode was reduced by 12%. Figure 15 similarly compares and shows the 5.6 GHz antisymmetric mode reduced by 32%. Examination of electric field at other points in the simulation showed similar reduction of these modes. This satisfies our goal of selectively attenuating the antisymmetric model.

SOS VERSION: JANUARY 1986 DATE: 5-JUN-86
SIMULATION: CCTWT86-19

TIME HISTORY PLOT
MAGNITUDE OF FFT OF E3 COMPONENT
AT COORDINATE (5,1,21)

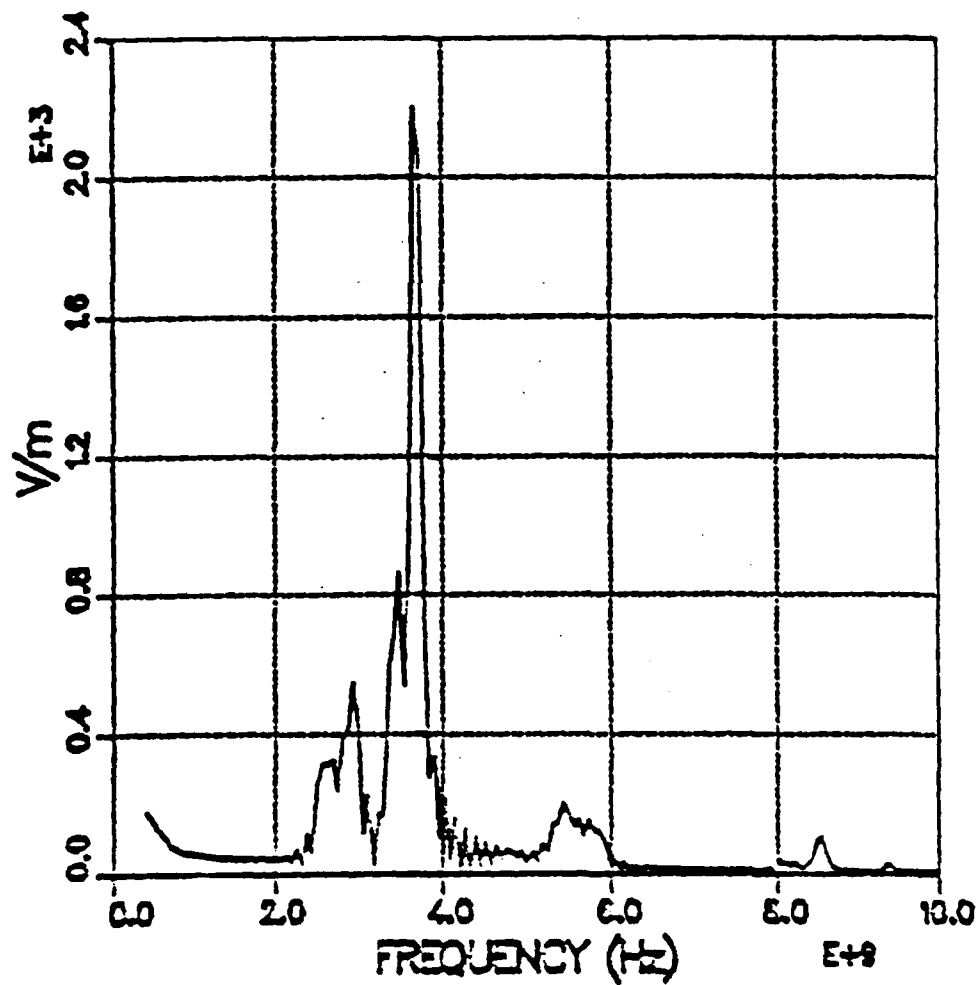


Figure 14. Fourier Transform from Symmetric CCTWT with Membrane Dampers

SOS VERSION: JANUARY 1985 DATE: 4-JUN-85
SIMULATION: CCTWT86-18

TIME HISTORY PLOT
MAGNITUDE OF FFT OF E3 COMPONENT
AT COORDINATE (5,1,21)

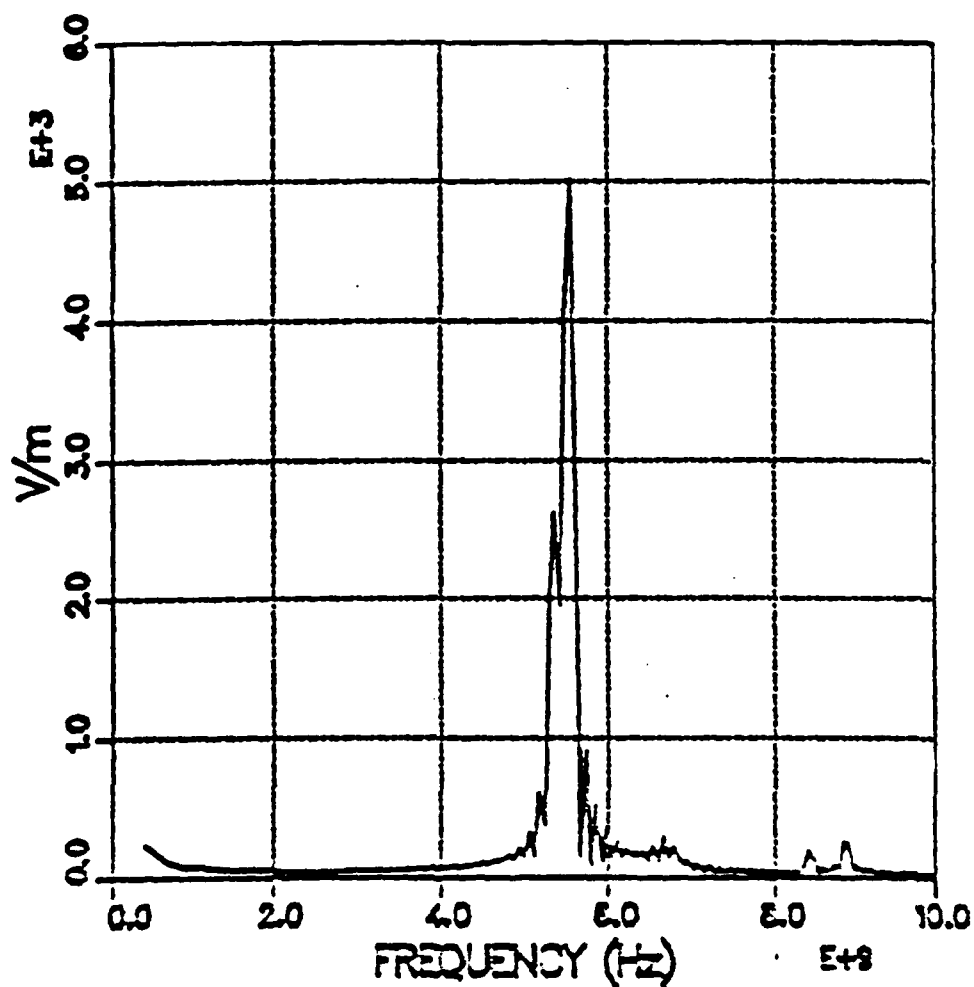


Figure 15. Fourier Transform from Antisymmetric CCTWT with Membrane Dampers

SECTION 3

PROGRAM PLAN

3.1 KEY TECHNICAL ISSUES

In our original proposal, we identified a number of key technical issues which would require consideration and resolution in designing coldtest software. These issues, described below, appear relevant today.

- Static and transient solutions each have advantages and limitations. Static solutions will provide mode structure, but will not generalize to transient hot test. Transient solutions provide everything (at possibly greater expense), but are more difficult to analyze in design terms. If both are pursued, should a single code result?
- There exist previous as well as on-going programs which have relevance. For example, sub-grid methods developed for the electromagnetic pulse community may be relevant to coldtest drivers as well as fine structural features of the tube. Work is underway on a three-dimensional eigenfunction code which may be applicable to static solutions. The Program should draw from these and other programs to exploit the existing technology base.
- Finite-difference and finite-element methods are substantially different. Finite-element grids can adapt to virtually any geometric shape, but establishing a grid in three dimensions requires a sophisticated generator, meshes are difficult to interpret and correct, and the method requires bookkeeping complexity. Finite-difference is simpler, but limited generally to conformal geometries.

- Interactive, user-friendly systems are generally believed conducive to computer-aided design. However, there is a trade-off between friendliness and protection - i.e., should a user be helped to do anything he wishes, or should he be protected from actions which the code considers in error?
- Efficiency is also an important issue in codes that will see extensive use. However, there is usually a trade-off between computational efficiency and personnel efficiency (user/maintenance/modification) which must be considered.
- The selection of computer may have important implications for mode of use, maintenance, and future modification and development. Cray computers are the most powerful, and are typically accessed remotely through Government agencies. Smaller mainframes, such as the VAX, are more readily accessible by users, but may require excessive run times. The choice of computer may also affect code logic and even the choice of algorithm.

3.2 OVERVIEW OF PLANNED DESIGN SYSTEM

In their User Requirements Report (Reference 4), Varian has attempted to detail and prioritize the needs of the user community for an rf circuit design code. This code represents the most immediate need. However, we believe that it is equally important to address the computer-aided design process in this initial effort. We believe that the approach to design, indeed, even the ways that specific codes are applied, must evolve over time. Therefore, the sooner we begin to address the entire problem, the faster the evolution will occur.

We are proposing to initiate work on five separate software modules:

- (1) Circuit Specification
- (2) Mesh Generator
- (3) Pre-Processor
- (4) Simulation Codes
- (5) Post-Processor

Each of these software modules will be discussed in detail below. This ambitious undertaking will be possible only by making certain compromises and by making use of certain existing software. For example, for the mesh generator, we recommend restricting the initial development to rectangular meshes in locally orthogonal systems (Cartesian and cylindrical). This does not allow the flexibility or accuracy of a triangular grid. However, it is achievable within the scope of the present effort and this will result in rapid experience with the system as a whole. It can be augmented with additional mesh generating algorithms as the system evolves.

With regard to choice of computer, we believe that simulation codes should, so far as practical, be designed to work on VAX and Cray computers. Both of the codes discussed below (Section 3.2.4) would clearly do so. However, all of the other modules would run on VAX, or if possible, PC-class machines such as the IBM-AT. The basic idea is that the modules would be interactive and menu driven.

3.2.1 Circuit Specification

As we envision it, the circuit specification module will provide the means for specifying structural elements of a circuit. We have already had some experience with this. The SOS code (Reference 5) presently contains a geometry generator, which allows the user to input simple generic shapes (rectangular, cylindrical, and spherical conductors) at arbitrary positions and orientations. The input data required by SOS is illustrated in Figure 4.4. In addition to perfect conductors, an "inversion" option can be used to indicate that the specified element represents a volume of space

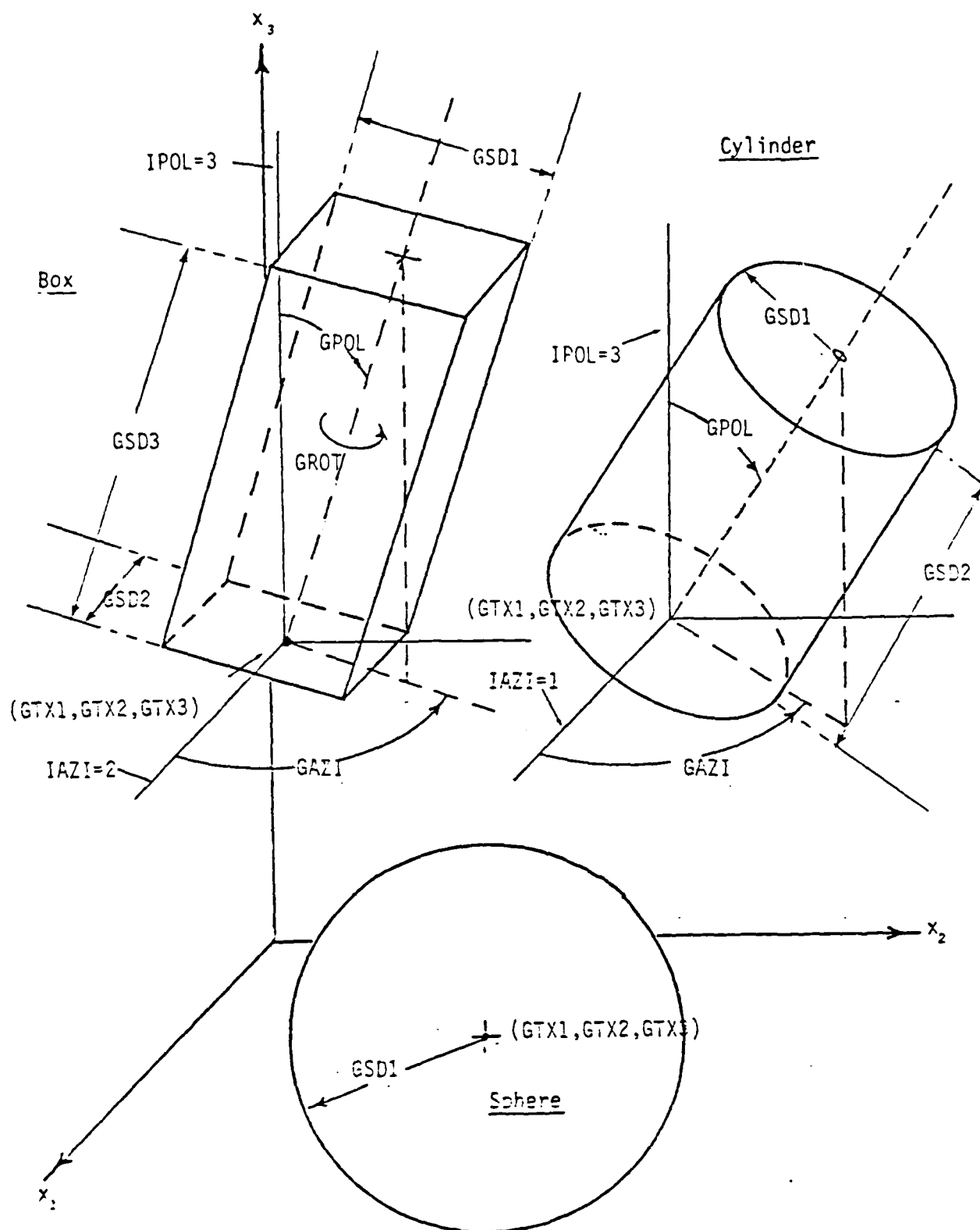


Figure 16. Generated Geometries in SOS

to be emptied of all solid structure. Thus, a block of perfect conductor created by one element can be numerically "machined" by subsequent elements using the inversion option.

We propose to remove this algorithm from SOS, and to generalize it to include all generic shapes, materials, and parametric dependences that are needed to specify a circuit for modeling purposes. Two- and three-dimensional graphics algorithms can be used to visually inspect the circuit.

Note that no mesh generation or modeling would be performed in this module. The intention is simply to allow specification of all relevant features of an actual or hypothetical circuit design, and to permanently store this information for subsequent use by a mesh generator or for future modification. As the design system evolves, it is likely that this algorithm will be replaced with an existing or yet-to-be developed algorithm which can encompass more of the manufacturer's needs, such as drafting, etc.

3.2.2 Mesh Generator

As explained previously, we propose initially to develop a mesh generator which will produce a quasi-rectangular grid in locally orthogonal (i.e., Cartesian and cylindrical) coordinate systems. This module will access data from the circuit specification module, and provide interactive graphics displays of the circuit and the mesh as it is developed by the user. It will also provide certain checks for interval consistency, monotonicity, enclosed boundaries, and so forth.

Once again, we can adapt an existing algorithm from the SOS code. This is the linear-quadratic functional prescription which is applied over a limited region of space. Working with one dimension and a limited region, the user can supply certain constraints and parameters, from which the grid will be generated and displayed graphically. Moving to the next adjacent region, the generator will assure continuity and conservation (if required),

and the process is repeated. This continues until the specification for each dimension is complete. Once the mesh has been generated, it can be stored for eventual use by one of the simulation codes.

3.2.3 Pre-Processor

The purpose of the mesh generator will be to process data for use by one of the simulation codes. Some of this data will be accessed from the circuit specification and mesh generator files. The remaining data will be furnished by the user, and may depend upon individual simulation requirements. For example, if the user elects to perform a time-dependent simulation, then he will need to furnish information on the cable frequency, the location of measurements, and so forth. The pre-processor will take data from all sources, and convert it to the form required by the simulation code. This conversion would normally include re-formatting, but could also include physical units conversion, and so forth. Thus, the main object of the pre-processor is to obtain information from existing files and from the user, and to convert it to a form recognizable by one of the simulation codes. Once obtained, this information also can be stored so that the process need not be repeated in future simulations. As we envision it, the pre-processor would also initiate the actual simulation.

3.2.4 Simulation Codes

This module would consist of a library of simulation codes, each of which is capable of addressing some facet of circuit operation. For example, it could contain codes to study mechanical response, thermal distributions, coldtest, hottest, and so forth. As we envision it, each code would be capable of "stand-alone" operation or of being accessed through the pre-processor (as part of the design system). Thus, it would be possible to add an existing code (such as MAGIC) simply by building the appropriate interface for the pre-processor.

It appears that two codes would provide useful coldtest capability. These are the time-dependent and eigenfunction codes, both in three-dimensions. For the time-dependent code, we propose a reduced (electromagnetic) version of the SOS code, which has been demonstrated previously (Reference 2) and in the present report (Section 2). Aside from desired simplification, the major change would be to the "sector" structure, which would be modified to use volumes of arbitrary thickness instead of planes as a unit of storage. This will allow simulation of irregular geometry, such as the rf feed on an amplifier circuit, at minimal computational expense.

In spite of the demonstrated success of the time-dependent codes, we believe that a three-dimensional eigenfunction code should be developed. From the standpoint of the user's time, the eigenfunction approach is likely to be more efficient. However, the two codes would provide different kinds of information, and thus would complement each other. For example, both codes can provide resonance information, and the pure eigenfunction distribution would aid mode identification in the transient analysis. In principle, the same mesh generation and diagnostic capabilities can be made available to both.

3.2.5 Post-Processor

We envision the role of the post-processor to be analogous to that of the pre-processor. That is, it would access and operate on data files produced by one of many simulation codes. In effect, it would provide commonality in output in the same way that the pre-processor provides commonality in input.

The post-processor would contain a library of output algorithms to be interactively selected and exercised by the user. This approach would provide access to the most powerful output algorithms in one place, and would make them available to all simulations. Obvious candidates for library algorithms include the following:

three-dimensional plots
contour plots
vector plots
time histories
FFT analysis (filter options)

It is expected that the library of algorithms will grow with time and experience. For the present, we can provide all of the algorithms simply by removing them from existing codes.

REFERENCES

1. P.E. Prince, "A Three Dimensional Plasma Simulation Code Applied to Phase Velocity Prediction in a Coupled Cavity Circuit," Technical Report AFTER-7, February 1, 1985 (Microwave Device and Physical Electronics Laboratory, Department of Electrical Engineering, University of Utah).
2. F. Friedlander, A. Karp, B. Gaiser, J. Gaiser, and B. Goplen, "Transient Analysis of Beam Interaction with Antisymmetric Mode in Truncated Periodic Structure Using 3-Dimensional Computer Code "SOS"," presented at 1985 IEEE International Electron Devices Meeting, Washington, D.C., 1-4 December 1985.
3. B. Goplen and R. Worl, "Numerical Simulations of a Monotron Oscillator Cavity and a Coupled-Cavity Travelling Wave Tube," Mission Research Corporation Report, MRC/WDC-R-098, July 1985.
4. F. Friedlander, "User Requirements Report," unpublished Varian report, May 1986.
5. B. Goplen, R. J. Barker, R. E. Clark, and J. McDonald, "User's Manual for SOS/Version-September 1983," Mission Research Corporation Report, MRC/WDC-R-065, September 1983.

END

11-86

DT/C